Escola de Camins
Escola Tècnica Superior d'Enginyeria de Camins, Canals i Ports
UPC BARCELONATECH

TREBALL FINAL DE MÀSTER

Estudio sobre la interacción flector-cortante en perfiles estructurales de acero

Study on bending-shear interaction in structural steel cross-sections

Treball realitzat per:
Adrià Jiménez Torres

Dirigit per:
Enrique Mirambell Arrizabalaga
Itsaso Arrayago Luquin

Màster en:
Enginyeria de Camins, Canals i Ports

Barcelona, 14/06/2017

Departament d'enginyeria civil i ambiental

Acknowledgements

I would like to acknowledge the support given to all the steel structures department in UPC, especially to Enrique Mirambell and Itsaso Arrayago, without whom the completion of this MSc thesis as is would not have been possible. Also a very special thank you to Alfredo, Alex, Sara and all my family for everything you have done.

Abstract

The resistance of steel cross-sections is covered by Eurocode 3 in clause 6.2 of EN 1993-1-1 [1]. The bending-shear interaction design rules make use of a reduced yield stress in the web to account for the presence of shear. Recent studies like [2] suggest that the interaction rule in Eurocode 3 for class 1 and 2 cross-sections might be unconservative for cases with high levels of shear. This MSc thesis presents the model developed in order to investigate bending-shear interaction by means of the finite element software *Abaqus* and the results obtained from the analysis. Five HEA and five IPE sections have been simulated with different spans to obtain different shear solicitation ratios V/V_{pl}. The influence of the yield stress and the presence or lack of strain-hardening of the steel is also investigated. The yield stresses considered are $235N/mm^2$ and $355N/mm^2$. The results obtained are compared to the interaction rules in EN 1993-1-1 [1], NEN 6770 [3], DIN 18800 [4] and also the interaction rule in EN 1993-1-1 [1] but adopting the web area as the shear area of the section.

Resumen

La resistencia de las secciones de acero se presenta en el Eurocódigo 3 en el artículo 6.2 en la norma EN 1993-1-1 [1]. Las reglas de interacción flector-cortante utilizan un límite elástico reducido en el alma para tener en cuenta la presencia del esfuerzo cortante. Estudios recientes como [2] sugieren que la interacción en el Eudocódigo 3 para secciones transversales clase 1 y 2 podría ser insegura para casos con altos niveles de esfuerzo cortante. En esta tesis de máster se presenta el modelo desarrollado para investigar la interacción flector-cortante con el software de elementos finitos *Abaqus* así como los resultados que se derivan del análisis. Cinco secciones HEA y cinco secciones IPE se han simulado con distintas luces para obtener diferentes grados de solicitación a cortante V/V_{pl}. También se investigan la influencia del límite elástico y de la presencia o ausencia del endurecimiento por deformación del acero. Los límites elásticos considerados son $235N/mm^2$ y $355N/mm^2$. Los resultados obtenidos se comparan con las reglas de interacción en las normas EN 1993-1-1 [1], NEN 6770 [3], DIN 18800 [4] así como la regla de interacción en EN 1993-1-1 [1] utilizando como área a cortante de la sección el área del alma.

Contents

Chapter 1

Introduction

It is a widely known fact that the resistance of a steel beam subjected to flexure is reduced when there is a substantial amount of shear force. This implies that beams which should achieve a certain resistance to bending moments M_{Rd} will not achieve that resistance due to the presence of shear.

Recent experimental results show that the formulas given in Eurocode 3 [1] on bending-shear interaction appear to be unconservative in some cases. In this MSc thesis, the main goal is to analyse this matter by means of the finite element code *Abaqus*. Extensive research has been done in this field, and many different expressions have been proposed to consider the effect of the bending-shear interaction.

One possibility is to use the well-known Von Mises yield criterion. Considering the stress-state of a beam subjected to flexure, the Von Mises failure criterion is represented by:

$$\sigma_{co,Ed} = \sqrt{\sigma_{x,Ed}^2 + 3\tau_{Ed}^2} \tag{1.1}$$

Obviously, in a general case with bending and shear there will be both normal and shear stresses in a section. This means that the Von Mises criterion always takes into account the presence of shear and limits the normal stresses (unlike many current standards do), and therefore, always reduces the bending resistance of the member. However, it appears that the Von Mises criterion is too conservative for low shear cases, when no reduction of the yield stress is appreciated, and less conservative than the interaction rule in EN 1993-1-1 [1] for high levels of shear. This motivates to find more accurate expressions to describe bending-shear interaction than eq. 1.1. Moreover, it is more convenient to find an expression in terms of forces rather than stresses for practical application purposes. Also, it may be possible to obtain more

optimistic interaction rules based on the section class depending on the slenderness of the plates conforming each type of beam.

The methodology used in the research presented in this thesis is widely used by many researchers. The usual procedure is to gather data by means of experimental results and/or numerical simulations. The experimental results are used to validate the finite element model. Once the model is validated it can be used to obtain a larger amount of data by means of parametric studies where the influence of the most relevant parameters can be observed and more general conclusions can be drawn. In this investigation, a study on bending-shear interaction is undertaken by using numerical simulations. The aims of this research are:

- To gather information about bending-shear interaction and its state of the art (articles, reports, design manuals, standards, etc.)
- To research in current norms and codes in order to evaluate and compare the existing rules to be considered when addressing the bending-shear interaction.
- To develop a numerical model to reproduce experimental tests of beams subjected to flexure considering different shear utilisation ratios and to validate the numerical model with experimental results.
- To undertake a parametric study to determine which parameters are the most impactful in the interaction between bending moment and shear force and to quantify such impact.
- To analyse the obtained results in the numerical simulations and obtain the ultimate loads in every studied case in accordance with a set of established criteria.
- To provide a proposal of design recommendations and draw conclusions with the information obtained from the simulations and the analysis of their results.

In order to fulfil these goals, this document is divided in the following sections:

- State of the art of bending-shear interaction: Overview of the experimental and numerical studies being undertaken currently and in depth discussion on previous rules and proposals by researchers. Discussion on the current norms in Europe (Eurocode 3 [1], DIN [4], NEN [3], EAE [5]) emphasising on the bending-shear interaction rule in EN 1993-1-1 [1].

- Numerical model: Detailed description of the developed model. Description and justification of the geometries studied, boundary conditions modelling and meshing. Failure criteria.
- Validation of the numerical model: Comparison of the developed model against experimental data and other simulated results.
- Parametric study: Determination of the impact of each of the parameters involved in the problem (L, A_v, f_y, etc.). Quantification of such impact.
- Results and analysis: Display of all the results obtained. Analysis of the results and discussion. Design recommendations.
- Summary and conclusions.
- References.

Chapter 2

State of the art

2.1 Previous studies on bending-shear interaction

The theoretical background of the bending-shear interaction is the assumption that shear is only carried by the web. This means that the flanges will always be able to reach their yield stress f_y at yield while the web might not (depending on the shear force in the section). This phenomenon reduces the bending resistance of the web which ultimately reduces the bending resistance of the section.

Most of the research on this matter is quite old, often referred to sections with slender webs for bridges where the thickness of the web is reduced as much as possible. In this situation it is important to determine the bending resistance accounting for shear, bearing in mind that the plastic shear resistance might not be achieved due to local buckling of the web due to shear stresses in the slender web. The first force-based formulation of the bending-shear interaction for plate girders was proposed by Basler [6] in 1961. A slightly modified version of that equation was then introduced in the Eurocode:

$$\frac{M}{M_{pl,Rd}} + \left(1 - \frac{M_{f,Rd}}{M_{pl,Rd}}\right)\left(\frac{2V}{V_{bw,Rd}} - 1\right)^2 \leq 1.0 \quad if\, M < M_{c,Rd} \tag{2.1}$$

where:
-$M_{f,Rd}$ is the plastic moment resistance of the section consisting of the effective area of the flanges.
-$M_{pl,Rd}$ is the plastic resistance of the cross-section irrespective of the class of the section.
-$M_{c,Rd}$ is the bending resistance of the section according to its section class.

-$V_{bw,Rd}$ is the shear buckling resistance of the web panel (or plastic shear resistance, whichever is smaller).
-M, V are the values of the applied bending moment and shear force on the section.
It can be observed that Basler's proposal (eq. 2.1) [6] always takes into account the influence of the shear force.

In 1971 Fujii et al. [7] developed a tri-linear interaction diagram considering the flange contribution to the shear resistance as well. In 1974 Herzog [8] developed similar interaction model as Fujii et al. (eq. 2.2) [7]. Further force-based M-V interaction equations were developed by Shahabian and Roberts in 1999 [9] and in 2008 [10] (eqs. 2.2 and 2.3). Two different equations are proposed for the M-V interaction behaviour of I-girders with slender web. These two formulas are given in chronological order.

$$\left(\frac{M}{M_u}\right)^4 + \frac{V}{V_u} \leq 1.0 \tag{2.2}$$

$$\left(\frac{M}{M_u}\right)^4 + \left(\frac{V}{V_u}\right)^4 \leq 1.0 \tag{2.3}$$

where M_u and V_u are the ultimate resistances to bending and shear force, respectively.

Sinur and Beg [11] investigated the bending-shear interaction behaviour of I-girders with longitudinally stiffened web. According to their numerical results the proposal of EN1993-1-5 [12] was modified in form of the following equation, where k is recommended to be set to 1.0.

$$\frac{M}{M_{el,eff,Rd}} + \left(1 - \frac{M_{f,Rd}}{M_{el,eff,Rd}}\right)\left(\frac{2V}{V_{bw,Rd}} - 1\right)^k \leq 1.0 \quad if\, V > 0.5V_{bw,Rd} \tag{2.4}$$

where $M_{el,eff,Rd}$ is the elastic or effective moment resistance of the section, depending on its section class. This equation is very similar to that in the Eurocode with the difference that it uses the design elastic bending moment resistance depending on the cross-section class instead of the plastic moment capacity $M_{pl,Rd}$. Also, Braun and Kuhlmann [13] proposed an interaction equation for bending, shear and patch loading for I-girders with flat web. The equation is as follows:

$$\left(\frac{M}{M_{pl,Rd}}\right)^{3.6} + \left(\frac{V - 0.5F}{V_{bw,Rd}}\right)^{1.6} + \frac{F}{F_{Rd}} \leq 1.0 \quad with\, M \leq M_{c,Rd} \tag{2.5}$$

where $F_R d$ is the patch loading resistances of the investigated girder.

Lee et al. [14] revised the proposal of the AASHTO [15] and AISC [16] specification for M-V interaction behaviour and proposed a modified version. The proposed design method considers the ratio of the web and flange cross-sectional areas in the M-V interaction behaviour following the eqs. 2.6 and 2.7:

$$\frac{V}{V_u} = 0.5 + 0.28\lambda \tag{2.6}$$

$$\lambda = \sqrt{3 - \frac{12}{A_w/A_f}\left[\left(1 + \frac{A_w/A_f}{4}\right)\frac{M}{M_u} - 1\right]} \tag{2.7}$$

Where A_w and A_f are the web and flange cross-sectional areas. The steel resistance of cross-sections is covered by Eurocode 3 in clause 6.2 of EN 1993-1-1 [1]. As it has been said before, it is a common procedure to consider that the shear force is carried only by web, and the bending-shear interaction design rule makes use of a reduced yield stress in the shear area of the section to account for the presence of shear force. Subsequently, the reduced plastic bending moment is calculated for class 1 and class 2 cross-sections (for class 3 and 4 cross-sections, the Von Mises yield criterion must be used).

One of the most relevant studies performed recently is that undertaken by Dekker and Snijder [2]. It was observed that most of the research on bending-shear interaction is quite old, and some more research was necessary. In that study many available experimental results were compared to the interaction design rule in Eurocode 3. Fig. 2.1 shows the M/M_{pl} and V/V_{pl} ratios for many experimental test results in the literature and the interaction rule in EN 1993-1-1 [1]:

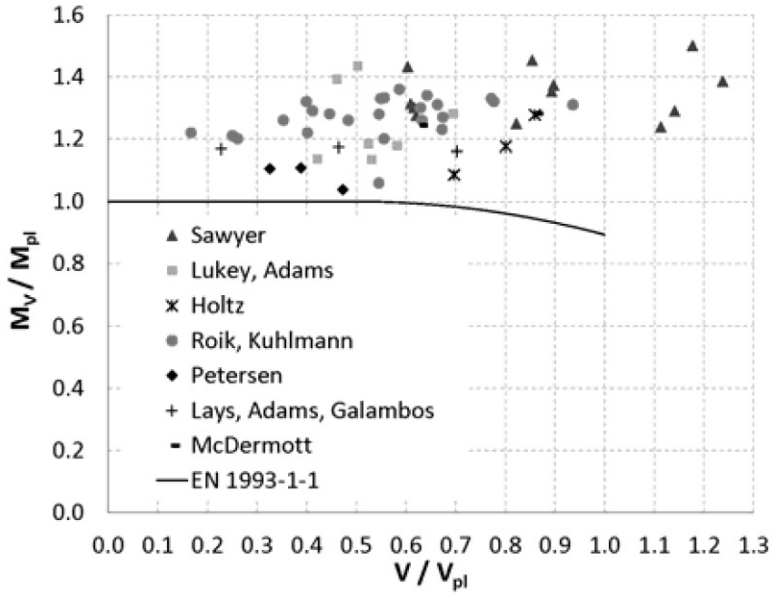

Figure 2.1: Experimental results gathered by Snijder and Dekker [2]

It appears that all these experiments are on the safe side. However, these results were performed only to research on section classification and not bending-shear interaction. Therefore, the results in fig. 2.1 are less valuable to study bending-shear interaction. Subsequently, some more experimental tests were performed.

The tests consisted of HEA240 beams belonging to one batch in steel S235JR. These were subjected to three-point bending until failure. Since it is expected that the steel properties vary over the section, coupons were taken from the flanges and web at several positions. Then the yield stress averaged to obtain a representative value for the whole section. The experimental failure loads obtained in the tests are compared to the interaction design rule in EN 1993-1-1 [1] considering an average yield stress for the whole section in one case (left graph in fig. 2.2) and different yield stresses for the flanges and web in another case (right graph in fig. 2.2). Although some small differences can be appreciated, it appears that the experimental results are unconservative for short specimens with high levels of shear force. On the other hand, the tests with shear levels not close to V_{pl} are very much on the safe side with a resisted bending moment much larger than M_{pl} in some cases:

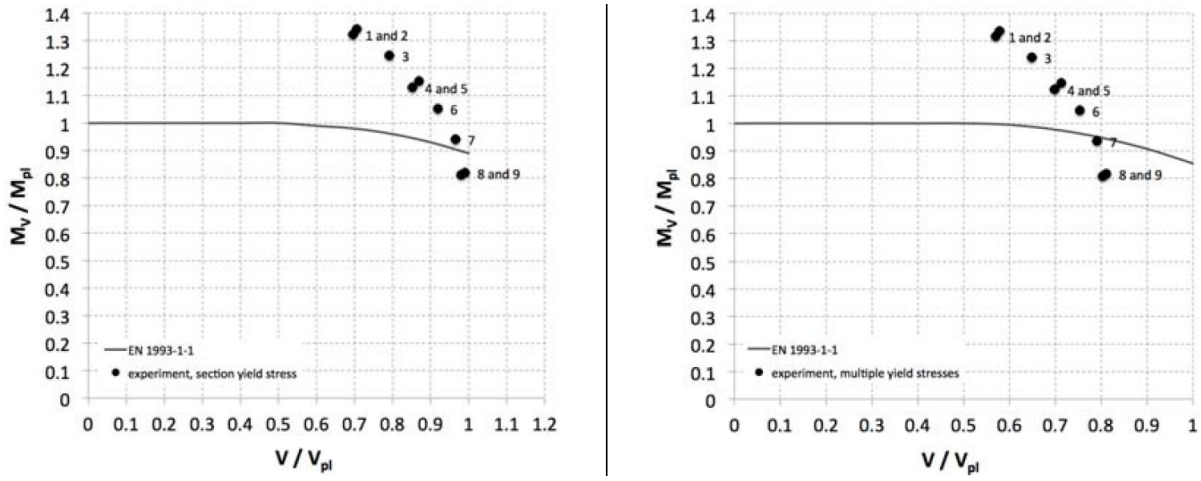

Figure 2.2: Experimental results from tests performed by Snijder and Dekker [2]

These experimental results suggest that the bending-shear interaction design rule of Eurocode 3 for I-sections might be unconservative for those cases where shear behaviour dominates. These results were used to validate a finite element model to continue the research on this subject.

Some more results obtained from more tests performed shortly after were also used to elaborate and validate a numerical model [17]. Several beam specimens were carefully measured in order to reproduce them with *Abaqus*. It is a known fact that steel beams have manufacturing tolerances, which entails that the depth of the section and the thickness of the web and flanges in the numerical model were variable across the section accounting for the imperfections of the beams. Once again, more coupon tests were performed to obtain the yield stress of the steel E, the yield stress f_y and the ultimate strength f_u of the specimens in several positions all over the section. Two specimens were reproduced with the finite element model.

The simulations were performed taking into account the geometric imperfections in the beams and also the heterogeneous properties of the material over the section. For each steel profile studied, measurements at several positions were performed to reproduce the behaviour of the samples as realistically as possible. To reproduce a three-point bending test, rolling hinges were simulated at the supports, with a line of nodes constrained in such a way that could only rotate about the transverse axis of the beam. The midsection was constrained to avoid any longitudinal or transversal displacement, preventing any lateral-torsional problems. At midspan and at the supports, the stiffeners welded to the specimens were modelled. All these

simulations were undertaken by using solid 3D elements in order to reproduce the roots between flanges and web. The numerical results were then compared to the experimental results. The simulated tests seem to have a reduction of the bending resistance accounting for the presence of shear. However, the bending-shear design rule given in EN 1993-1-1 [1] seems to be safe in the cases studied in [17].

Another current study about bending-shear interaction in unstiffened I-girders has been elaborated by Jáger, Kövesdi and Dunai [18]. In this study, another numerical model is developed to study the failure mechanism of slender section when subjected to bending, shear and a combination of both. The material considered is an isotropic elastic-hardening plastic material up to its ultimate strength f_u, from where the material behaves as perfectly plastic. Geometrical imperfections were applied in accordance with the failure mechanism (web shear buckling or compression buckling due to flexure). With all the data from the simulations, an in-depth comparison is undertaken between the rules in EN 1993-1-1 [1] and EN 1993-1-5 [12] and the proposal from Sinur and Beg [11]. The main findings in such study were that the numerical results fit quite well the existing interaction rule for slender sections for bending moments up to 90% of the bending resistance of the section. For values over 90%, the shear resistance of the flanges is underestimated and the results are conservative. Also, it appears that the ratio between flanges area and the web area plays a significant role in the bending-shear interaction behaviour. For higher A_f/A_w ratios, the rule in EN 1993-1-5 [12] provides safe results. On the other hand, for lower A_f/A_w ratios, the rule in EN 1993-1-5 [12] is clearly unconservative, and the proposal from Sinur and Beg [11] provides safe results. However, the consideration of the flanges shear buckling resistance cannot be considered in all cases. It appears that for large A_f/A_w ratios it can lead to an unconservative design. The interaction rule proposed in the study is:

$$\frac{M}{M_{el,eff,Rd}} + \left(1 - \frac{M_{f,Rd}}{M_{el,eff,Rd}}\right)\left(\frac{2V}{V_{bw,Rd}} - 1\right)^k \leq 1.0 \quad if\ V > 0.5V_{bw,Rd} \tag{2.8}$$

with

$$k = \left(\frac{M_{f,Rd}}{M_{el,eff,Rd}} + 0.2\right)^{15} + 1 \tag{2.9}$$

Another recent study in this subject has been performed by Baláž and Koleková [19]. In that study, a deep comparison between different standards is presented and

the scope of the study extends not only to steel cross-sections but also to aluminium alloy sections. The result of their comparison is the following chart graph:

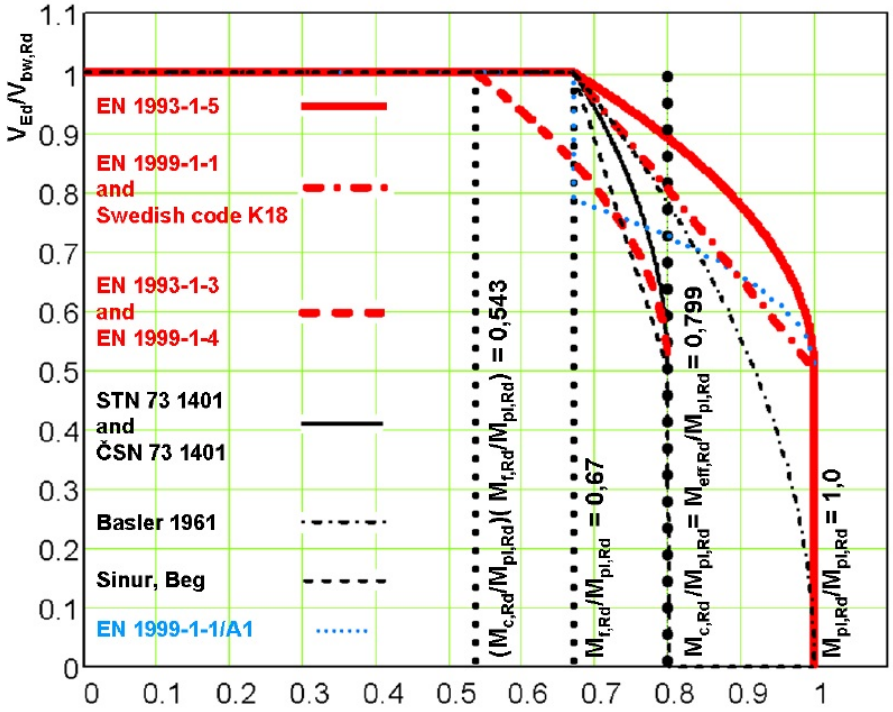

Figure 2.3: Comparison of several norms and studies by Baláž and Koleková [19]

It can easily be observed that Eurocode 3 is the most optimistic among all the interaction rules considered in fig. 2.3. The Swedish code K18 and Eurocode 9 also consider the interaction for $V_{Ed} \geq 0.5V_{pl,Rd}$ but not with a parabolic parameter but with a linear decrease of resistance down to $M_{f,Rd}$ when $V_{Ed} = V_{pl,Rd}$.

2.2 Bending-shear interaction in standards

Clause 6.2.8 of EN 1993-1-1 [1] states that the influence of shear on the major axis bending resistance is insignificant if the shear force is smaller than half of the plastic shear resistance of the section. If the shear force is larger than half of the plastic resistance, the yield strength in the shear area is reduced:

$$f_{y,r} = (1 - \rho) f_y \tag{2.10}$$

Where $f_{y,r}$ is the reduced yield stress, f_y is the nominal yield stress and ρ is the reduction factor to determine the reduced design values of the resistance to flexure allowing the presence of shear. The reduction parameter ρ is obtained as:

$$\rho = \left(\frac{2V}{V_{pl}} - 1 \right)^2 \tag{2.11}$$

Where V is the applied shear force and V_{pl} is the plastic shear resistance of the section:

$$V_{pl} = A_v f_y / \sqrt{3} \tag{2.12}$$

In the expression 2.12, A_v stands for the shear area of the section.
The shear area to be considered in the equation is what differs in several norms in Europe. The adoption of different shear areas gives as a result different shear plastic strengths, which lead to different reduced bending resistances $M_{V,Rd}$ accounting for the presence of shear. In figure 2.4 different shear areas can be observed.

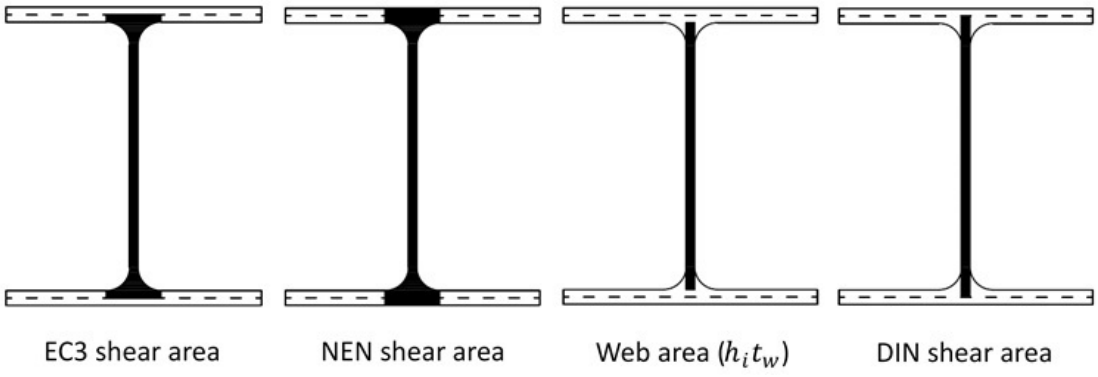

Figure 2.4: Shear area in EN 1993-1-1 [1], NEN 6770 [3], web area and shear area in DIN 18800 [4]

It seems obvious that the differences are substantial and can lead to different values

for V_{pl}. The reduced plastic resistance moment allowing for the presence of shear can also be obtained as:

$$M_{V,Rd} = \left[W_{pl} - \frac{\rho A_w^2}{4t_w} \right] f_y \tag{2.13}$$

Where W_{pl} is the plastic section modulus, t_w is the web thickness and A_w is the web area as shown in the figure above, extending till the flanges. Eq. 2.13 considers only the web area as the shear area and provides considerably more conservative results. Clause 6.2.1 of EN 1993-1-1 [1] gives the Von Mises yield criterion for a two-dimensional stress state. Reducing this criterion for combined normal and shear stresses only and subsequently rewriting in the form of a reduced yield stress results in:

$$f_{y,r} = \sqrt{1 - \left(\frac{V}{V_{pl}} \right)^2} \cdot f_y \tag{2.14}$$

This formula, compared to the other interaction expressions in 1993-1-1 [1] in the following figure, shows that the Von Mises reduced yield stress is sometimes greater and sometimes smaller than what the current interaction rule states:

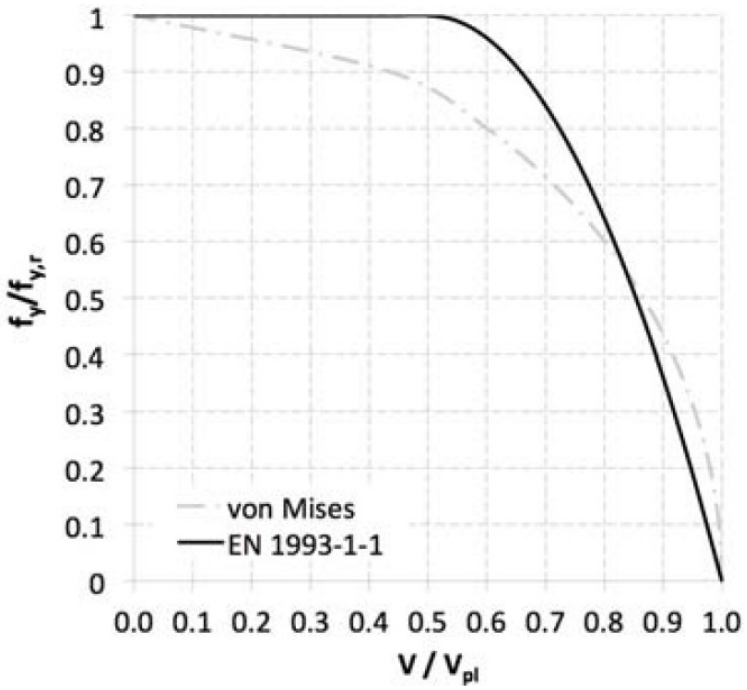

Figure 2.5: Comparison between the Von Mises yield criterion and the rule in EN 1993-1-1 [1] for the reduced yield stress $f_{y,r}$ by Snijder and Dekker [2]

According to DIN 18800 [4], the influence of a shear force on the bending resistance is taken into account if the shear force is greater than 33 percent of the plastic shear

resistance. The interaction design rule for bending moment and shear is:

$$0.88\frac{M}{M_{pl}} + 0.37\frac{V}{V_{pl}} \leq 1.0 \quad if\, V > 0.33V_{pl} \tag{2.15}$$

Which can be rewritten into:

$$M_V = \frac{M_{pl}}{0.88}\left(1 - 0.37\frac{V}{V_{pl}}\right) \quad if\, V > 0.33V_{pl} \tag{2.16}$$

It should be noted that in these expressions the shear area adopted extends to half way the flanges as indicated above. The former Dutch code NEN 6770 [3] gives similar rules as EN 1993-1-1 [1]. The only difference is the shear area used consequently throughout the bending-shear interaction design rule. The next figure shows the differences between the three design rules for a cross section HEA240 with shear force V on the horizontal axis, also indicating the influence of different shear areas. Fig. 2.6 distinguishes an absolute shear graph (on the left) and a normalised shear ratio V/V_{pl} (on the right). The differences are substantial.

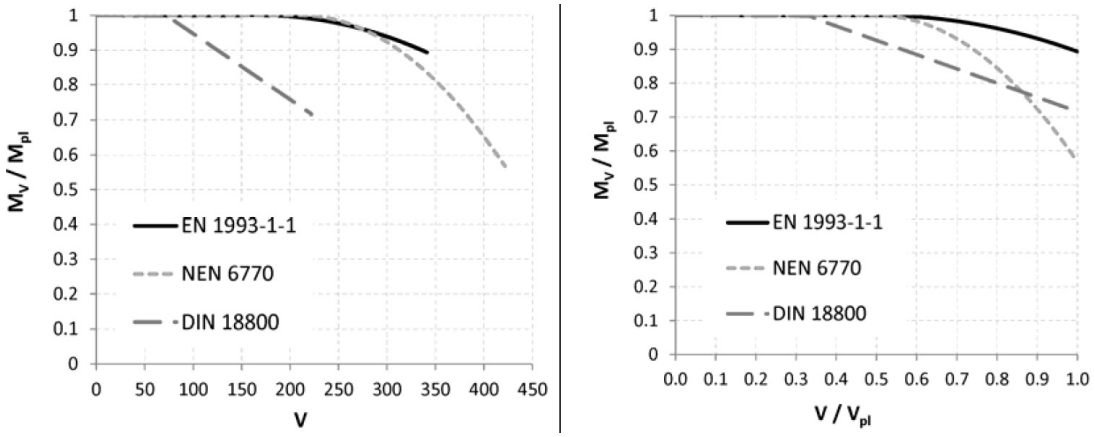

Figure 2.6: Comparison between different bending-shear interaction rules by Snijder and Dekker [2]

As it can be observed on the left graph in fig. 2.6, the largest shear area in NEN 6770 [3] provides a very large shear resistance. However, for high levels of shear, the ultimate bending capacity is lower to that of other standards. This is because all the shear area is used exclusively to carry shear force and the adoption of a larger shear area leaves a smaller spare cross-sectional area to resist bending moments.

Chapter 3

Numerical model

The software *Abaqus* was used in the simulations. It is a general-purpose finite-element analyser that employs implicit integration scheme [20]. The model consists of a simply supported beam subjected to three-point bending with a concentrated load at midspan. The midsection is studied to determine the failure load of the beam. A general static analysis approach was used in all the simulations since no instability phenomena are studied. The solution at each load increment was obtained by means of a direct full-Newton equation solver.

The simulations were performed with a maximum allowed number of load increments of up to 200 with a minimum load increment of 0.001% of the total load to be applied. The initial increment was set to 30% of the load. At such low levels of loading all the beam fibres are still in elastic regime and no plastification has been observed in any case. This allows to make a large initial increment without compromising any accuracy of the solution.

3.1 Geometries

Since the aim of this MSc thesis is to investigate on bending-shear interaction, the profiles studied are those which are most often used carrying combined flexure and shear loads. For that reason, the sections used in this study all belong to the HEA and IPE series. In order to study different A_v/A ratios (being A the total area of the section and A_v the shear area) the sections chosen in this study are IPE120, IPE240, IPE360, IPE500, IPE600, HEA120, HEA240, HEA360, HEA500 and HEA600. By selecting these profiles the whole range of section sizes is covered for the IPE and HEA families.

For each section, several different beams with variable lengths have been generated. In order to ensure a very significant amount of shear force, all the profiles have been simulated with spans ranging from $L = 5d$ (being d the nominal depth of the section) up to $L = 20d$ with little or no influence of the shear force when the failure of the beam is dominated by bending. In cases where little or no influence of shear is observed, fewer lengths have been modelled to avoid generating results that do not provide any useful information for this study. Fig. 3.1 shows the model of a HEA360 beam with span $L = 2700mm$:

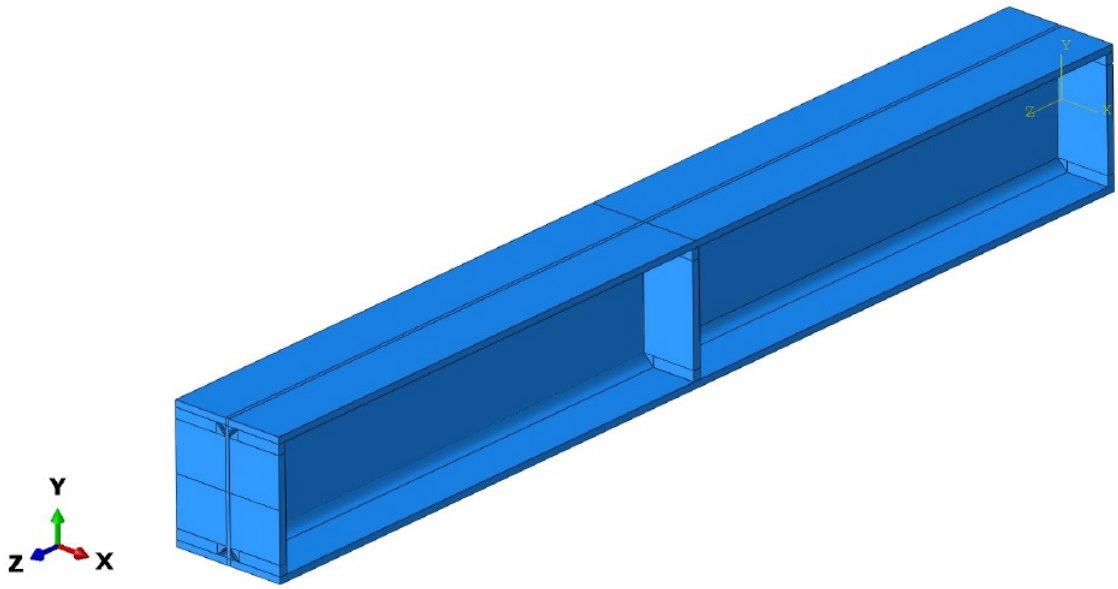

Figure 3.1: Geometry of an HEA360 section with span $L = 2700mm$

The beams have been modelled with no imperfections and have been perfectly extruded with their idealised nominal section dimensions and web and flange thicknesses. The roots have been modelled as well, since they play a very important role in the shear resistance of the section. At the supports and at midspan, a welded stiffener has been modelled with a thickness equal to double the web thickness to avoid any potential instability phenomena. All the stiffeners have weld access holes at the corners adjacent to the beam web in order to reproduce the real geometry as reliably as possible.

The load applied is a downward surface traction applied on the edges of the central stiffeners. In fig. 3.2 an HEA360 can be seen with the applied load:

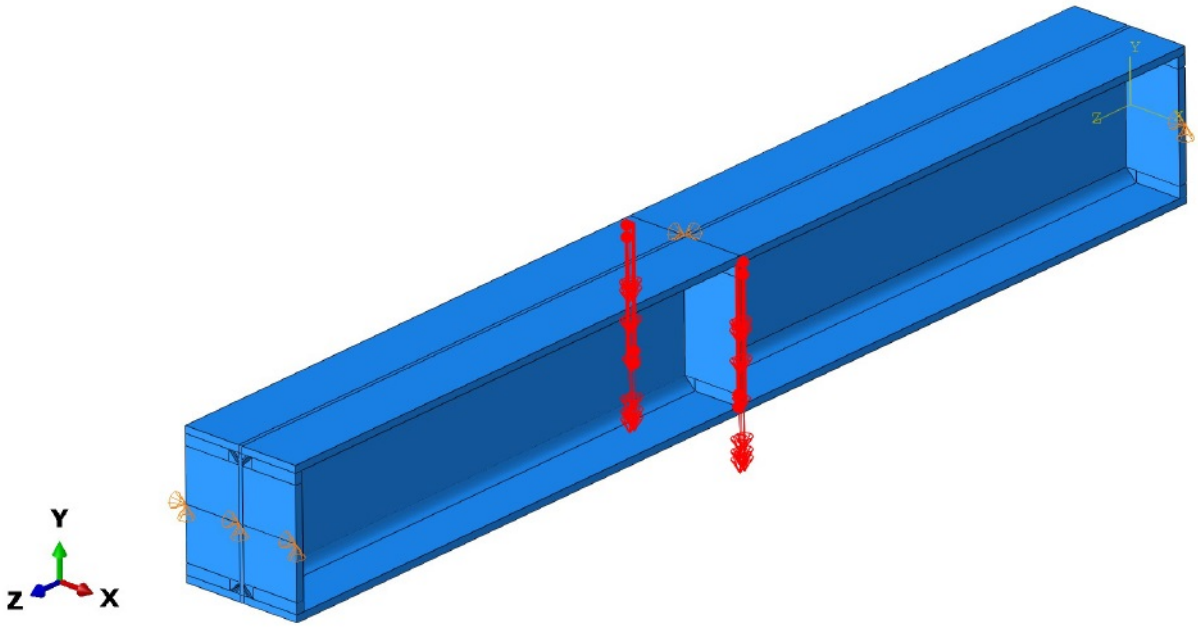

Figure 3.2: Load applied at the midsection of an HEA360. $L = 2700mm$

3.2 Meshing and boundary conditions

3.2.1 Meshing

In order to reproduce the roots that connect flanges and web it has been necessary to use solid 3D elements. The model has been meshed with reduced integration, linear hexahedral elements. After a mesh sensitivity check it was concluded that the use of higher order integrated elements provided the exact same results with a much higher computational cost. Two elements over the flange and web thicknesses proved to be sufficient. All the models have been meshed aiming for a good form factor of all elements (which has been particularly challenging for the root area). With this scheme, all simulations had a number of elements ranging from 51000 to 273000. In fig. 3.3 the meshing over the section of an HEA360 beam is displayed:

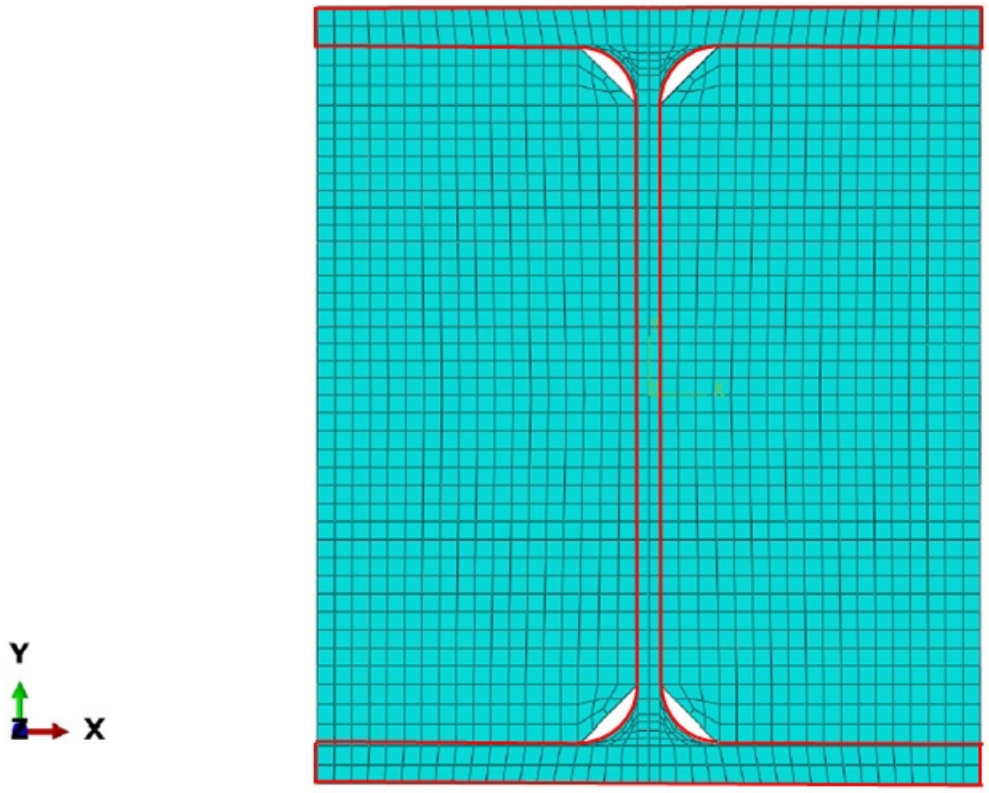

Figure 3.3: Section view of the mesh of an HEA360 profile (enclosed in red) and stiffeners

And in fig. 3.4 the mesh of a whole IPE120 beam with span $L = 600mm$ and the welded stiffeners is shown:

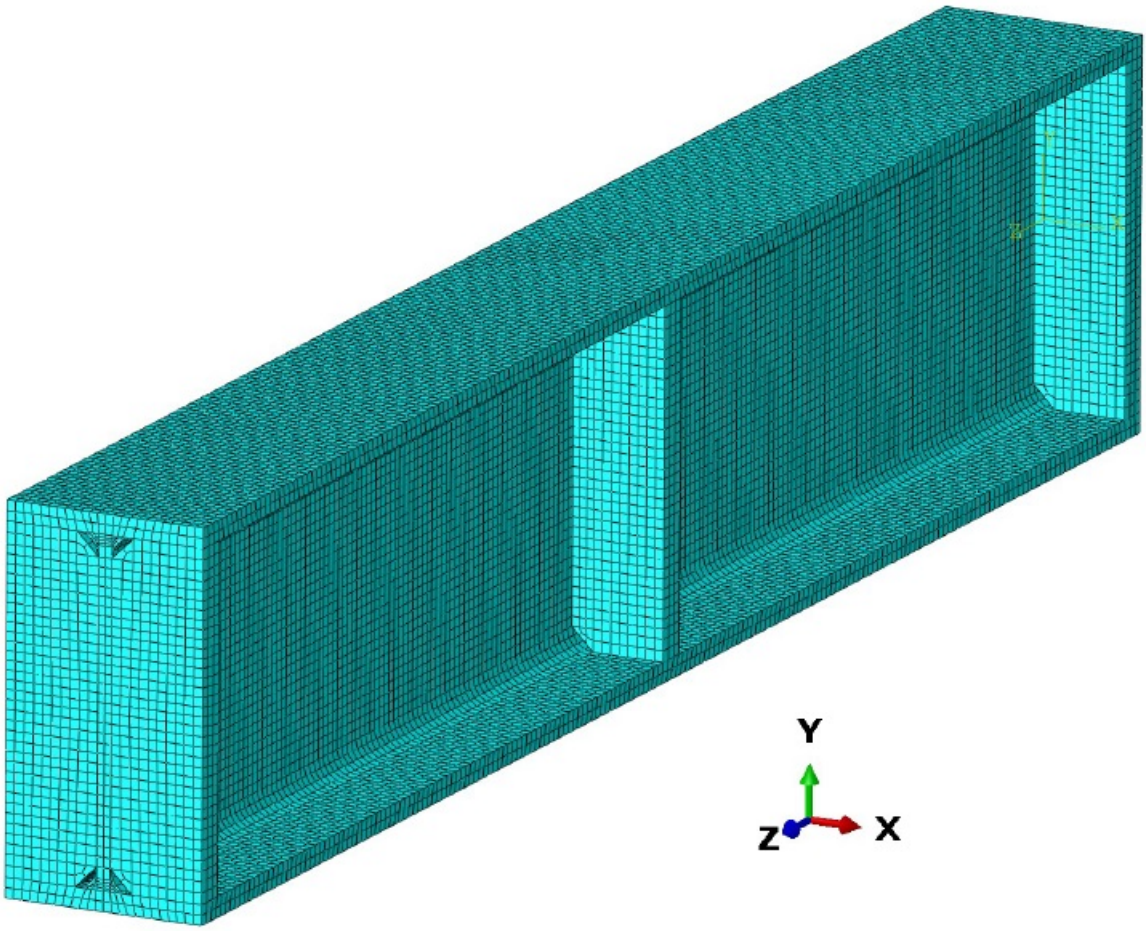

Figure 3.4: View of the mesh of an IPE120 beam with stiffeners

3.2.2 Boundary conditions

As it has been said before at the start of this chapter, all the models consist of I-beams subjected to three-point bending, thus carrying both flexure and shear forces only. In order to reproduce the simply supported behaviour of the beams in a three-point bending test, the supports of the beam were only allowed to rotate about the transversal axis of the beam (the strong axis of the section) and to move in the longitudinal direction. To do so, a line in the extreme sections of the beam was constrained and the X and Y displacements were not set free (see figs. 3.3 and 3.4 for sign criterion). These constraints avoided any rotation about the Y or Z axes. The beams were supported on a line at the center of gravity of the section and not on the bottom flange. This is because by supporting the beam on the center of gravity of the section its behaviour is more similar to the beam theory in elastic regime (which was used to validate the model). The boundary condition at the supports

can be seen in fig. 3.5:

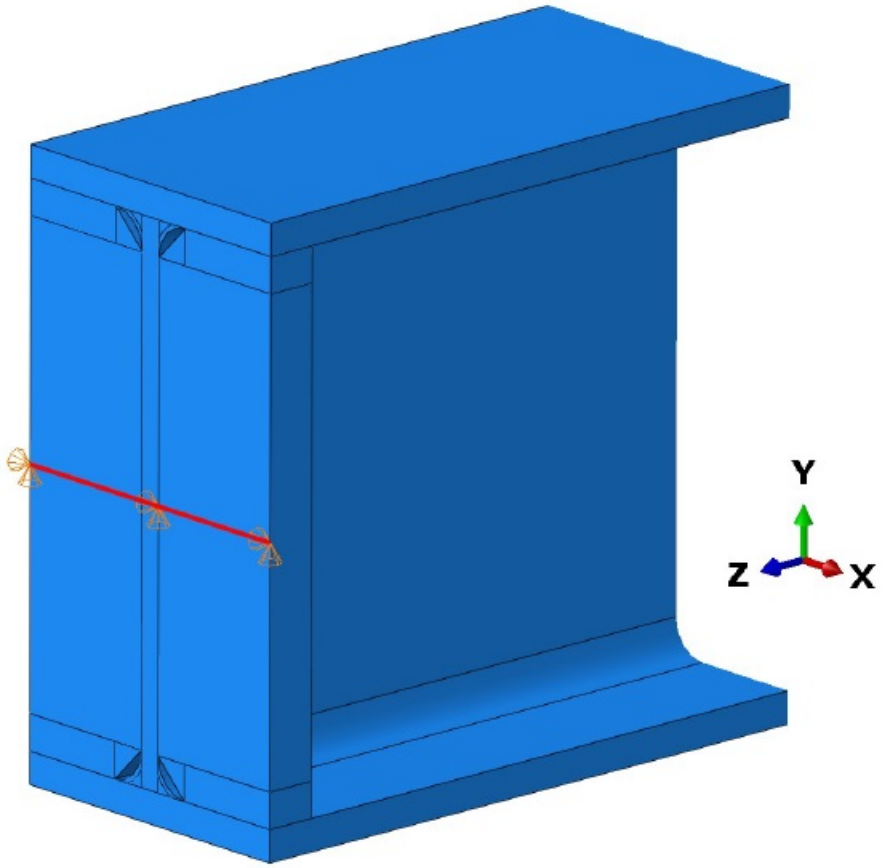

Figure 3.5: View of boundary conditions applied at the support. Transversal and vertical displacements are constrained

Since the supports can move freely in the longitudinal direction, the midsection needs to constrained in that regard. Also, any transversal displacements are constrained to avoid any lateral-torsional buckling problems that might arise otherwise. Only two symmetric points (one on the top flange, the other on the bottom flange) were constrained in the X and Z directions. The applied boundary conditions in the central section can be seen in fig. 3.6:

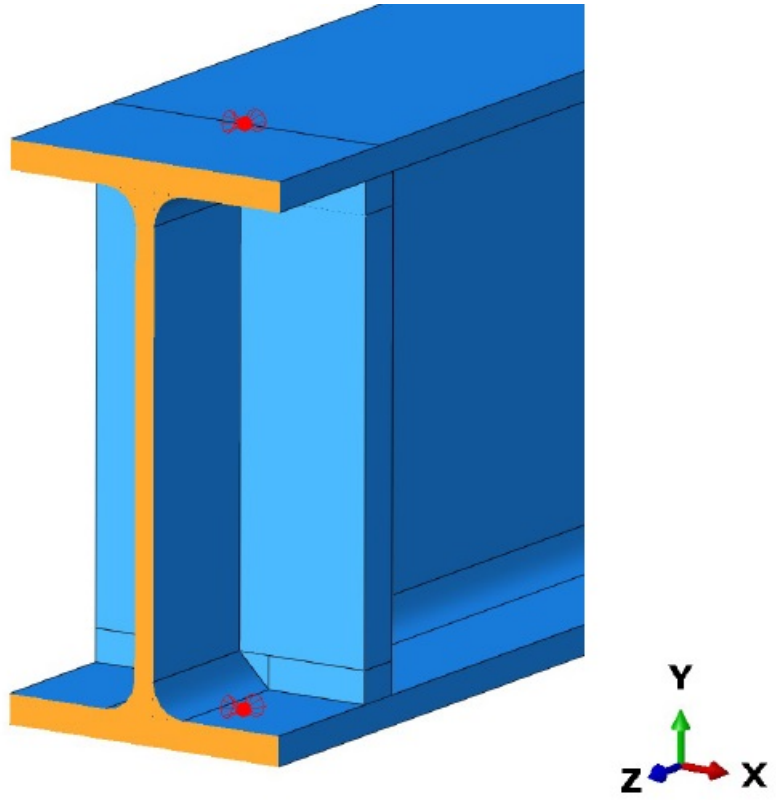

Figure 3.6: View of boundary conditions applied at the midsection. Transversal and longitudinal displacements are constrained

3.3 Failure criteria

In order to obtain the failure load in each simulated beam it is necessary to establish a set of failure criteria. In this study, the failure criteria has been established in terms of maximum allowable strains for the material. Different maximum allowable strains have been adopted for steels with strain-hardening or with perfect plasticity:

For the elastic-perfect plastic materials, with yield stress $f_y = 235N/mm^2$ and $f_y = 355N/mm^2$ the maximum allowable strain considered is $\varepsilon_{max} = 8\varepsilon_y$ with $\varepsilon_y = f_y/E$. Thus, the maximum allowable strain in perfect plastic steels is 8.95‰ for S235 and 13.52‰ for S355.

For the hardening plastic steels, the maximum allowable strains have been the ultimate strains of each steel at failure according to Yun and Gardner [21]. For steels grades S235 $\varepsilon_{max} = 20.83\%$ and for S355 $\varepsilon_{max} = 16.53\%$.

The choice of the maximum allowable strain in the hardening materials seems quite obvious. The criteria has been simply set to $\varepsilon_{max} = \varepsilon_u$. However, the choice of $\varepsilon_{max} = 8\varepsilon_y$ for non-hardening steels is somewhat more complex. It has been motivated by the fact that in the Spanish steel code EAE [5] the maximum allowable strain is $\varepsilon_{EAE,max} = 6\varepsilon_y$ for fibers carrying compression stresses in sections belonging to class 1 and 2. In order to ensure that the failure loads obtained in a load increment do not correspond to a stress concentration in a few elements, it has been considered that allowing slightly larger strains can lead to slightly more accurate results. However, it must be noted that at such levels of loading with several fibres of the beam with a Von Mises equivalent stress $\sigma_{co} \geq f_y$ small differences in strains lead to very minor load value changes.

In very short beams, shear strains can be much larger than bending strains. In these few cases, the maximum allowable shear strain has been considered to be $\gamma_{max} = \varepsilon_{max}/\sqrt{3}$. The adoption of this value is motivated by the Von Mises comparison stress: a similar expression has been adopted in terms of strains in order to limit the maximum allowable shear strains in the beams.

In fig. 3.7 there is an example. An HEA360 beam in steel S235 with hardening plastic behaviour with span $L = 2700mm$ $(L = 7.5d)$ is shown. At this particular load increment the beam has failed according to the above-mentioned established failure criteria. The maximum strain at this increment is $\varepsilon = 21.32\%$ and the maximum allowable strain for this steel is $\varepsilon_{max} = 20.83\%$. Therefore, it is considered that at this increment the beam has failed and the corresponding applied load is the ultimate load for this beam:

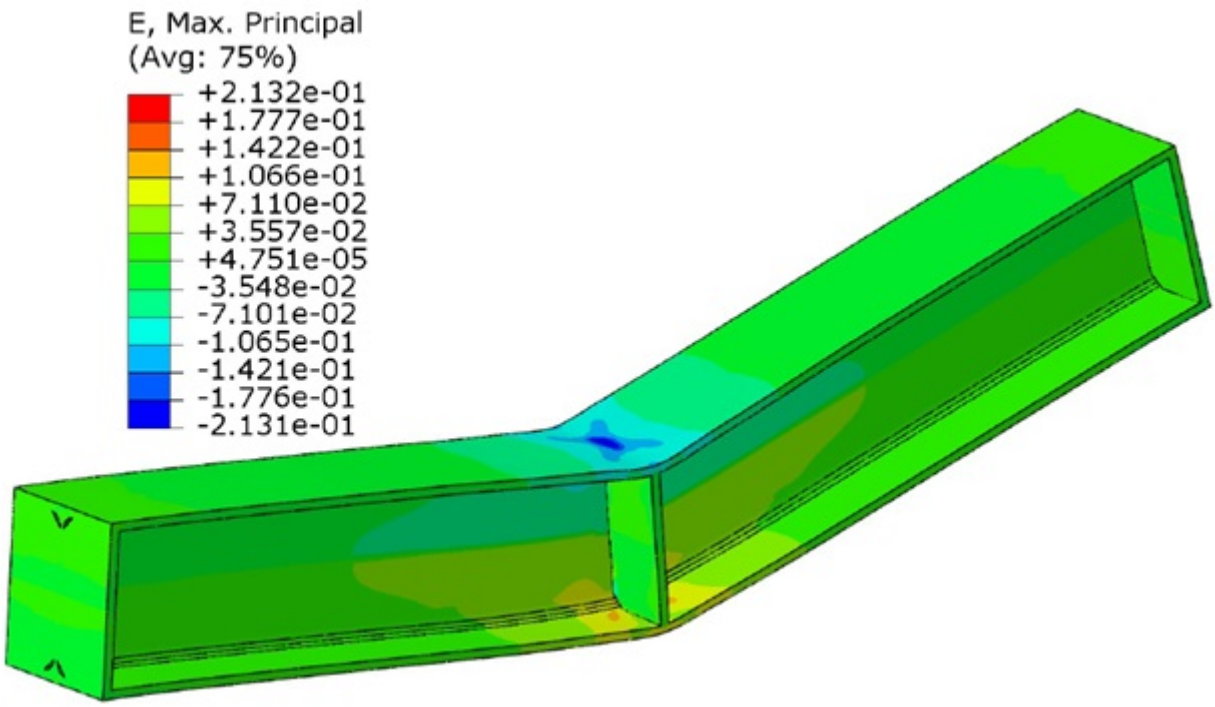

Figure 3.7: Strains on an HEA360 beam at failure. Span $L = 2700mm$

3.4 Validation of the model

In the first stages of the model, in order to validate its accuracy and reliability the obtained results in perfectly elastic regime were compared to the classical beam theory. In this first evaluation of the model deflections and stresses in several points of the section were compared. This was done at several sections for many beams. The results proved to be accurate within 1% to 2% of what the theory suggests.

After the initial check with a perfect elastic behaviour, the non-linear material properties were tested. In order to do so, two of the experimental tests performed by Snijder and Dekker [2] were reproduced. The tests consisted of simply supported beams subjected to three-point bending. The first consists of an HEA240 beam with span $L = 1950mm$ in steel S235. Since in the study it is reported that the measured yield limit of the steel is $f_y = 238N/mm^2$ the yield limit in the model was modified to match to the properties of the steel in the experimental test.

The obtained failure load in the simulation is $F_{u,FE} = 506kN$, whereas the mean experimental failure load is $F_{u,exp} = 484kN$. This means that the simulated failure load is 104.5% of the experimental failure load. The strains at failure are displayed in fig. 3.8:

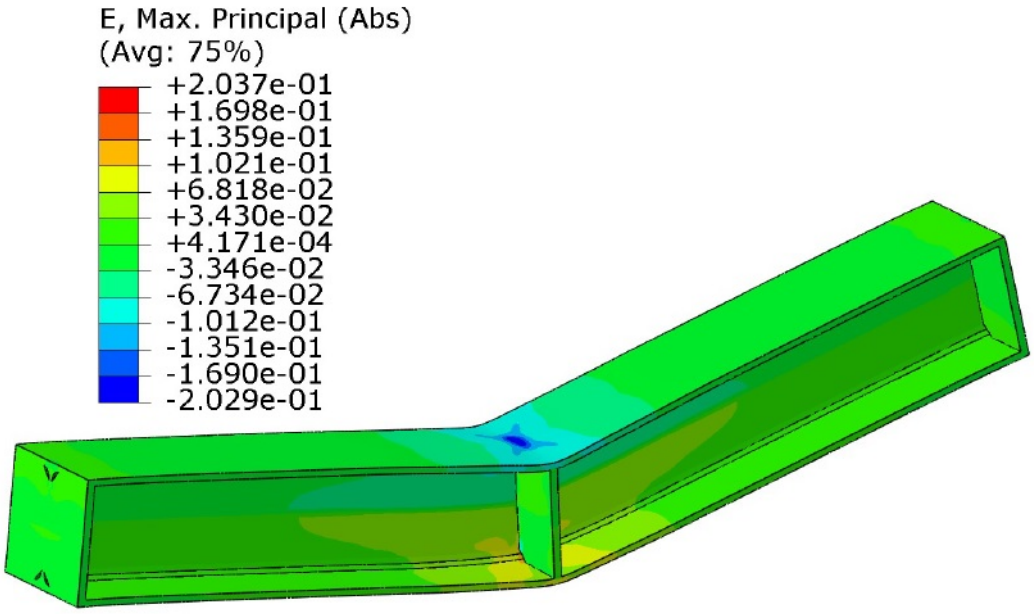

Figure 3.8: Principal strains on an HEA240 beam at failure ($F_{u,FE} = 506kN$). Span $L = 1950mm$

The next load increment leads to a strain much larger than 20.83% so this is the load increment in which the failure occurs according to our established failure criteria. It is also remarkable that shear strains are quite significant and concentrated in the web:

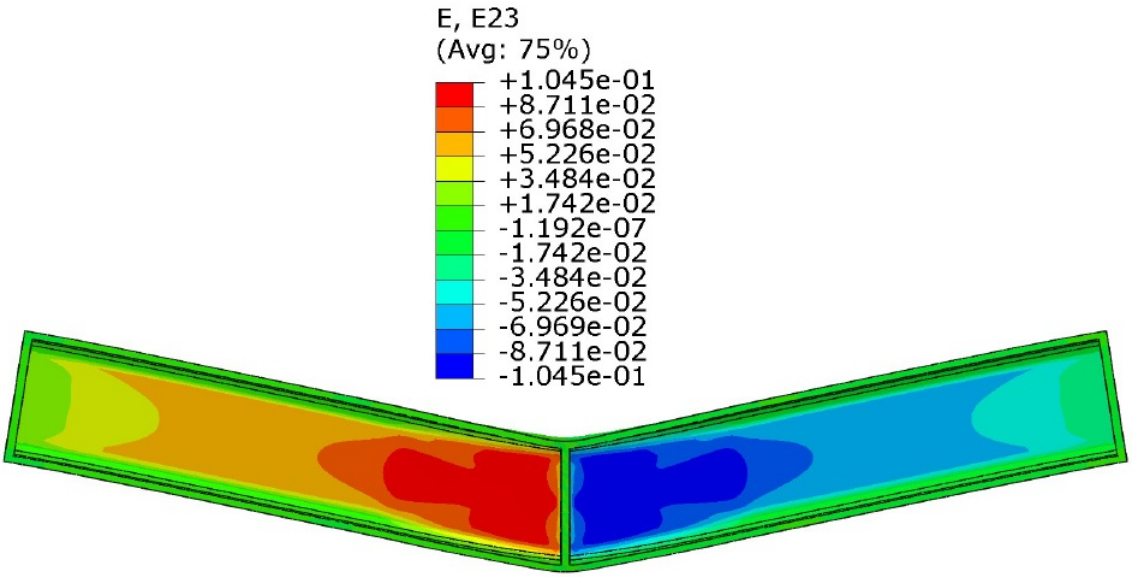

Figure 3.9: Shear strains on an HEA240 beam at failure ($F_{u,FE} = 506kN$). Span $L = 1950mm$

It is clear that a plastic hinge has formed in the midsection. In fig. 3.10 the Von Mises stress is represented:

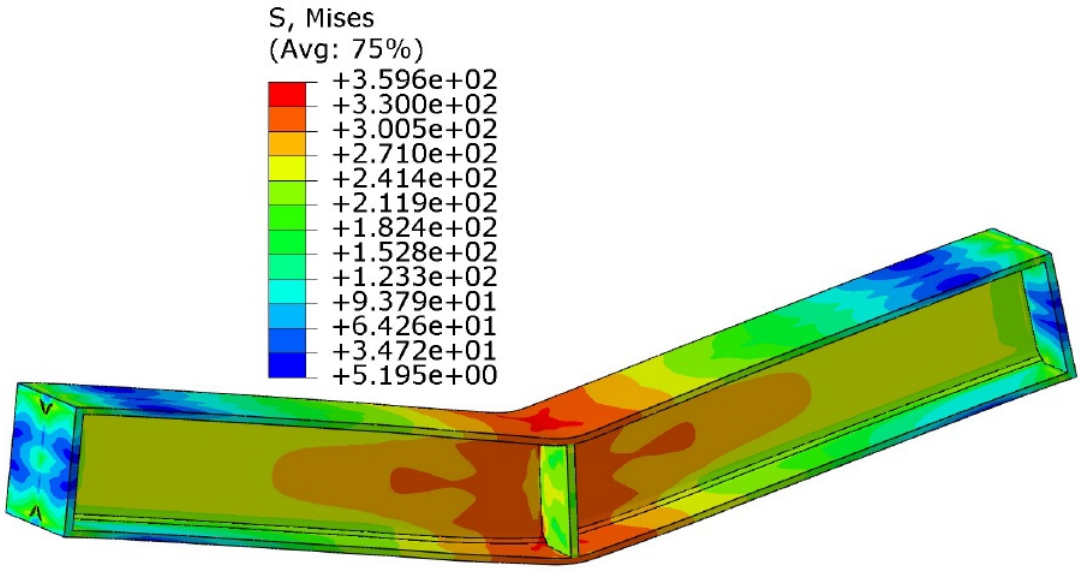

Figure 3.10: Von Mises stresses on an HEA240 beam at failure ($F_{u,FE} = 506kN$) in N/mm^2. Span $L = 1950mm$

It can be noted that all the areas in orange have a Von Mises stress over $300N/mm^2$, which indicates that those fibers are undergoing large strains. Fig. 3.11 shows all the elements in plastic regime at failure (in red):

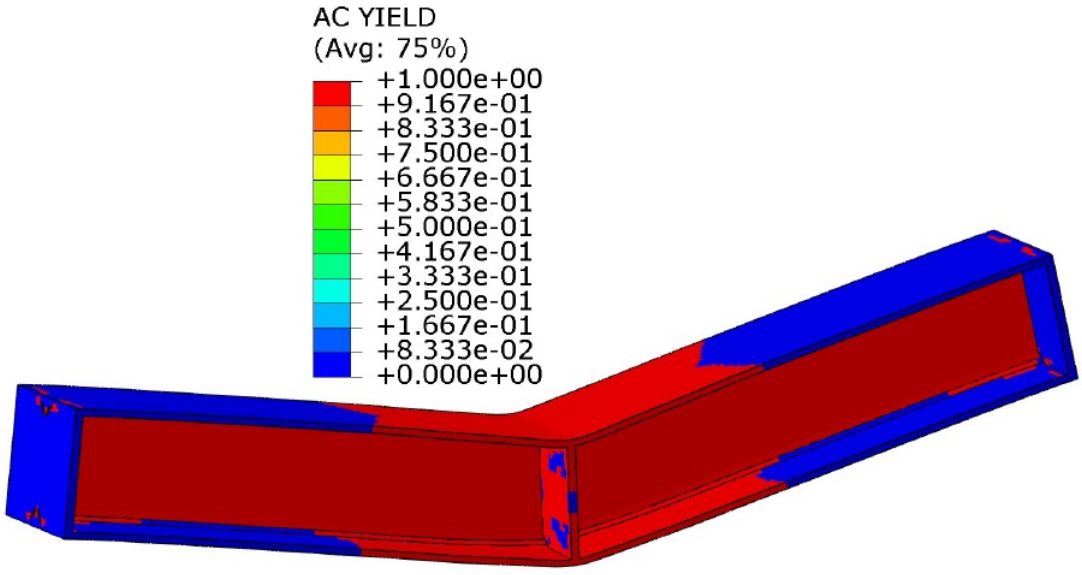

Figure 3.11: Yielded fibers on an HEA240 beam at failure ($F_{u,FE} = 506kN$). Span $L = 1950mm$

And as it can be expected, deflections under such circumstances are quite large. The maximum deflection at the middle of the beam is $u_{max} = 193.6mm$ which is a bit

less than the depth of the beam. Therefore the beam has developed a plastic hinge with large deformations concentrated around the midsection. The hinge is clearly noticeable by the shape of the deformed beam:

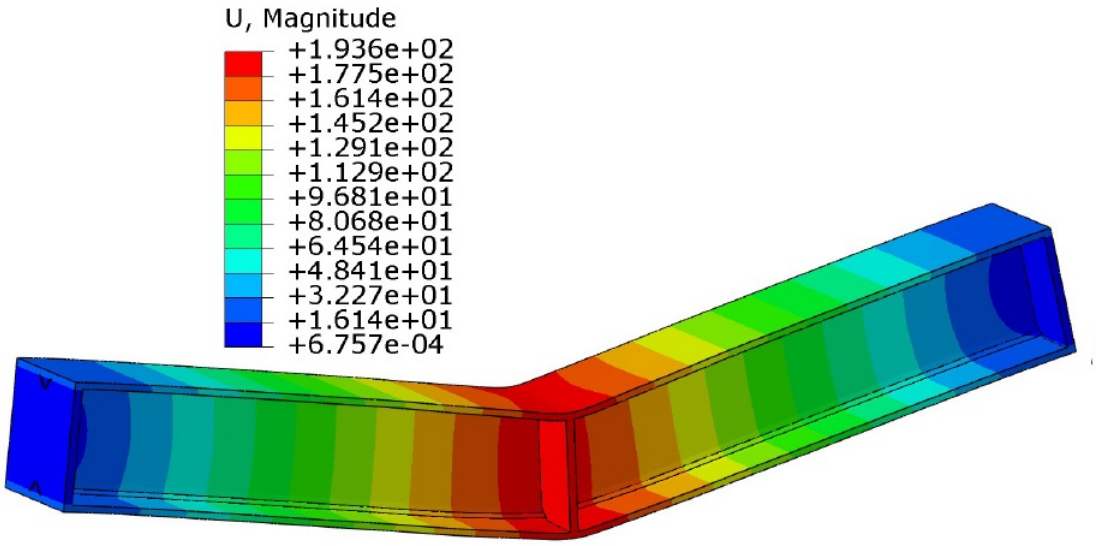

Figure 3.12: Displacements on an HEA240 beam at failure ($F_{u,FE} = 506kN$) in mm. Span $L = 1950mm$

For the second experiment, another HEA240 beam was tested with span $L = 1360mm$. The obtained failure load in the simulation is $F_{u,FE} = 574kN$, whereas the mean experimental failure load is $F_{u,exp} = 596kN$. This means that the simulated failure load is 96.3% of the experimental failure load. The strains at failure are displayed in fig. 3.13:

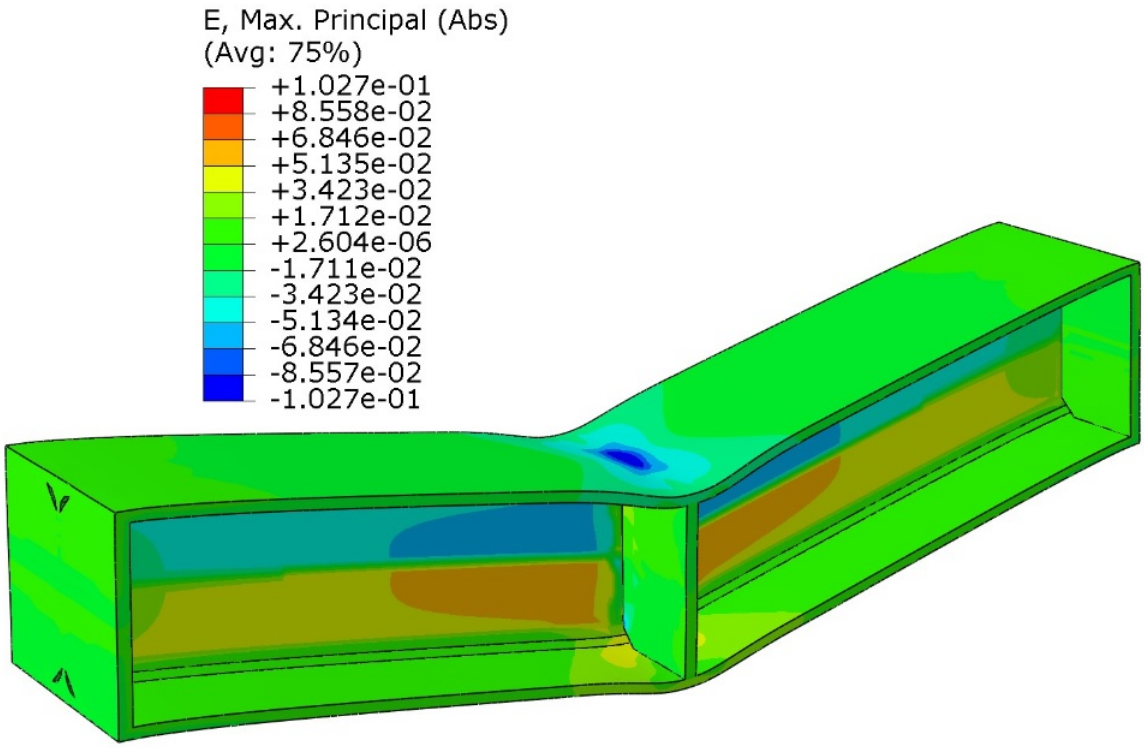

Figure 3.13: Principal strains on an HEA240 beam at failure ($F_{u,FE} = 574kN$). Span $L = 1360mm$

In the flanges, strains are not close to the ultimate strain. However, shear strains are very large:

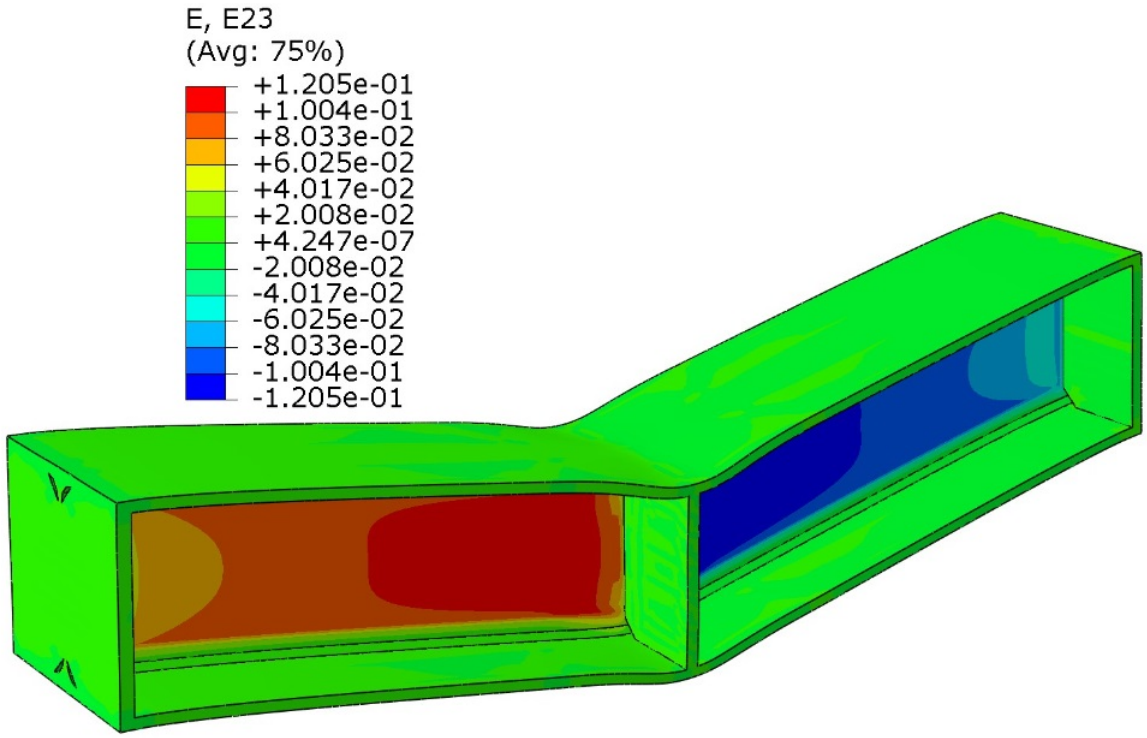

Figure 3.14: Shear strains on an HEA240 beam at failure ($F_{u,FE} = 574kN$). Span $L = 1360mm$

And at this step the maximum allowable shear stress is reached. In fig. 3.15 the Von Mises stress is represented:

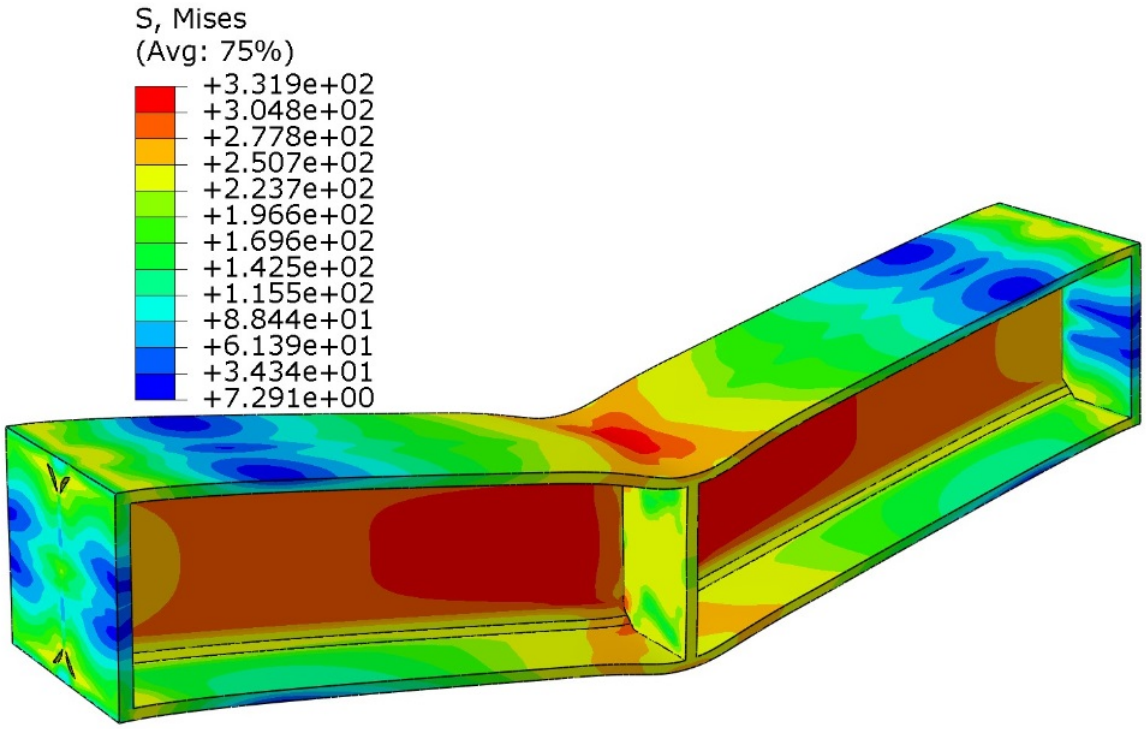

Figure 3.15: Von Mises stresses on an HEA240 beam at failure ($F_{u,FE} = 574kN$) in N/mm^2. Span $L = 1360mm$

It can be noted that all the areas in dark orange and red have a Von Mises stress over $277N/mm^2$, which indicates that those fibers are undergoing large strains. It can be observed that the shortest beam has a larger area in the web with high Von Mises comparison stresses, which indicates a higher influence of shear in its failure mechanism. Fig. 3.16 shows all the elements in plastic regime at failure (in red):

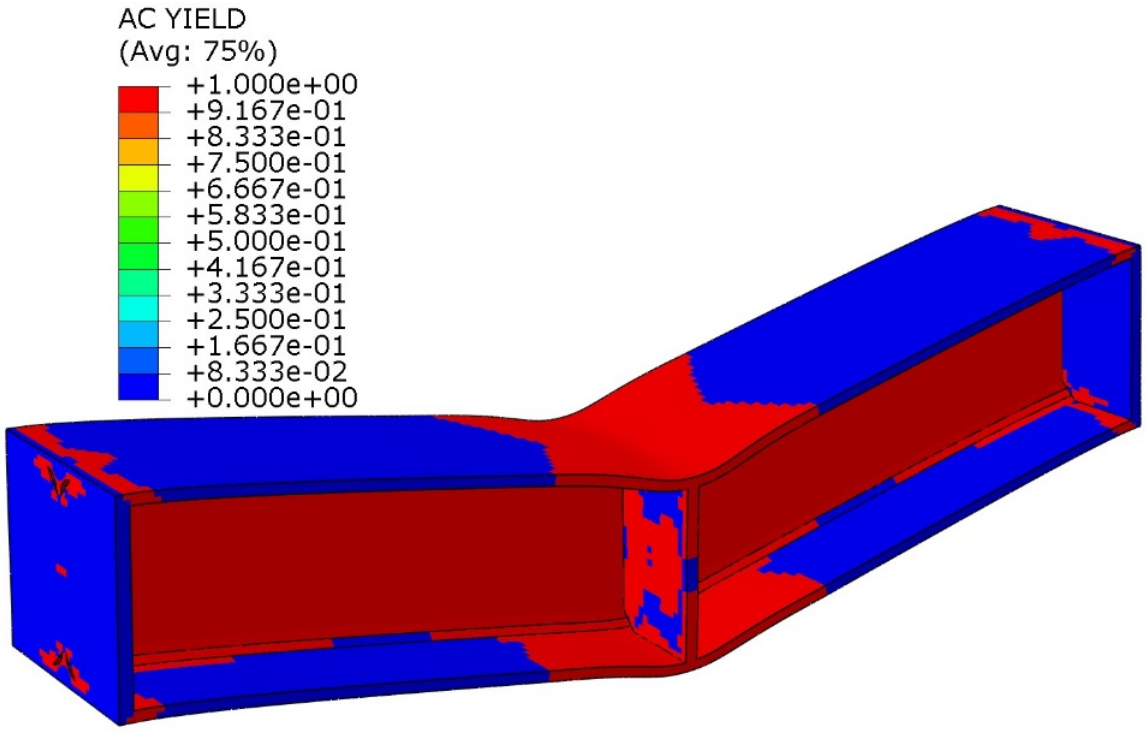

Figure 3.16: Yielded fibers on an HEA240 beam at failure ($F_{u,FE} = 574kN$). Span $L = 1360mm$

As happened with the longer beam, all the web is yielded and around the central section the flanges have yielded as well, indicating the formation of a plastic hinge in the midsection. And as it can be expected, deflections under such circumstances are quite large:

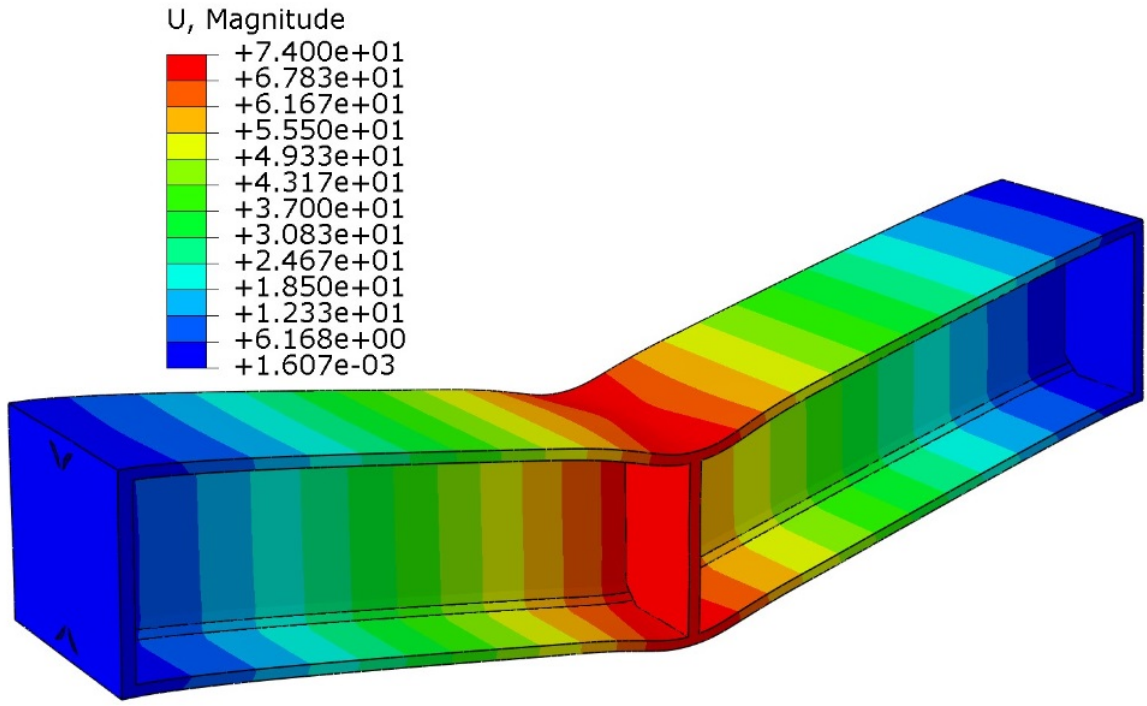

Figure 3.17: Displacements on an HEA240 beam at failure ($F_{u,FE} = 574kN$) in mm. Span $L = 1360mm$

The maximum displacement is $u_{max} = 74mm$ which is around $L/18$. Such large displacements appear when a plastic hinge has formed, as is the case.

With the data extracted from these two simulations to validate the model, the following results have been obtained:

Table 3.1: Comparison between the experimental tests in [2] (averaged) and simulated tests. All results in m and kN. yield stress $f_y = 238N/mm^2$

L		F_u	M_{exp}	V_{exp}	M_{exp}/M_{pl}	V_{exp}/V_{pl}
$1950mm$	Tests 1 and 2 (avg)	484	236	242	1.33	0.70
	Simulated test	506	247	253	1.39	0.73
$1360mm$	Tests 4 and 5 (avg)	596	203	298	1.14	0.86
	Simulated test	574	195	287	1.10	0.83

As it can be seen in table 3.1 the simulated results are quite close to the average of the two experimental tests performed in each case by Snijder and Dekker [2].

Another comparison with the results obtained for the validation of the model is

displayed in fig. 3.18, where the average of the experimental results and the simulated results are shown:

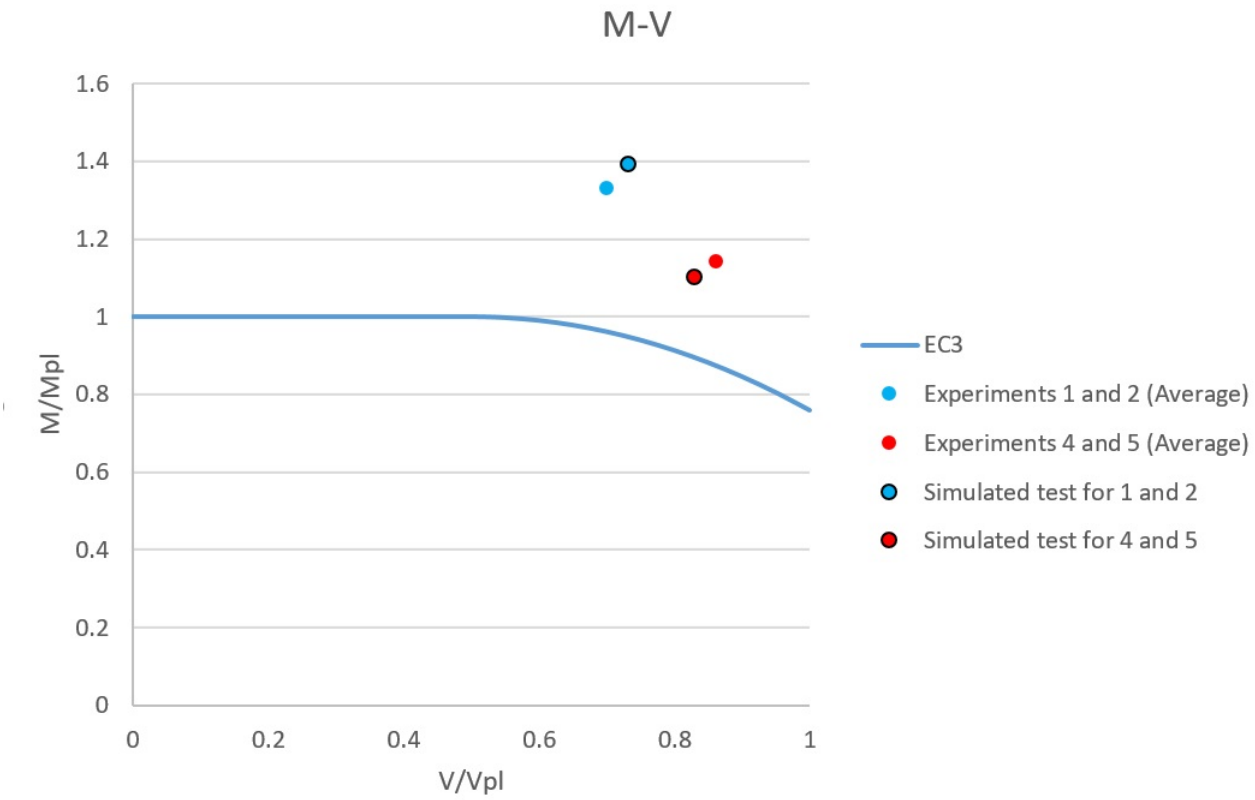

Figure 3.18: Comparison between simulated tests and experimental results in [2] and interaction rule in EN 1993-1-1 [1]

As it could be expected from the data in table 3.1 the values are quite close. It should be noted that the values representing the experimental results are averages, and the actual tests for each beam in [2] also present a small dispersion.

Therefore, these comparisons demonstrate that the derived numerical analyses are capable of accurately predicting the ultimate loads, the full experimental histories and the failure modes of steel beams subjected to three-point bending tests.

Chapter 4

Parametric study

Bending and shear are a pair of forces acting on a beam that appear at the same time when a point load is applied. Usually, the behaviour of the beam responds to a bending mechanism, where shear plays a minor part. However, it is not always the case and it is possible that the shear force is significant. Different ratios of shear and bending utilisation ratios lead to the necessity to quantify the influence of each parameter that contributes toward a bending or a shear resisting mechanism of the beam. In order to investigate bending-shear interaction with a wide range of different parameters, a total number of 172 simulations have been performed.

4.1 Geometric parameters

Due to the different natures of bending and shear it is obvious that some parameters will have more influence on either one or the other. For instance, the span of the beam L definitely has a tremendous impact on the interaction. Therefore, if the same load is applied to two simply supported beams one having longer span than the other, the longer one will present a more bending-dominated behaviour than the other. The longer the beam, the less load it can carry due to larger moments being applied. For very short beams, the behaviour could even be shear-dominant with little or no influence of flexure since the shear force remains constant under a certain load irrespective of beam span.

Since the beam span L may well be the parameter of largest importance in the bending-shear interaction, for every beam section several different lengths have been simulated ranging from $5d$ up to $20d$. Beam spans over $20d$ will not entail any shear

interaction with bending, since the bending moments will be very high and the failure mechanism will be exclusively due to bending. On the other hand, beams shorter that $5d$ are so short that shear deformation is much larger than bending deformation and the failure mechanism will be due exclusively to shear. Moreover, such a short specimen cannot be considered a beam, and a 3D general continuum mechanics approach should be considered since no beam theory applies to such case.

Another parameter that can have a large influence on the bending-shear interaction is the shear area of the section A_v or the ratio between the shear and total cross-sectional areas A_v/A. Larger webs provide larger shear resistances which means that under a certain point load larger webs will lead to lower shear utilisation ratios. That is why 5 different section sizes have been simulated for both IPE and HEA profile series. Larger profiles have smaller flanges compared to the whole area of the section, which may translate into a different behaviour from smaller profiles (where the flanges are comparatively larger).
For the HEA profile series a total of 5 different sections have been simulated. The spans of the beams simulated are (ranging from $5d$ to $20d$):

- HEA120: 600mm, 900mm, 1200mm, 1800mm and 2400mm.
- HEA240: 1400mm, 1800mm, 2200mm, 3000mm and 4800mm.
- HEA360: 1800mm, 2700mm, 3600mm, 5400mm and 7200mm.
- HEA500: 2500mm, 3750mm, 5000mm, 7500mm and 10000mm.
- HEA600: 3000mm, 4000mm, 5600mm, 9000mm and 12000mm.

For the IPE profile series a total of 5 different sections have been simulated. The spans of the beams simulated are:

- IPE120: 600mm, 900mm, 1200mm, 1800mm and 2400mm.
- IPE240: 1200mm, 1800mm, 2400mm, 3600mm.
- IPE360: 1800mm, 2700mm, and 3600mm.
- IPE500: 2500mm, 3750mm and 5000mm.
- IPE600: 3000mm, 4000mm and 6000mm.

Also, in order to compute the plastic resistance of a given section, the considered shear area has a very substantial impact (see fig. 2.4). In order to interpretate the results, three different shear areas considered in several standards are shown (EN 1993-1-1 [1], DIN 18800 [4] and NEN 6770 [3]) and the web area is also considered. It is very noticeable that the shear areas in the Dutch code NEN [3] and in the German norm DIN 18800 [4] will result in very different plastic shear resistances, with the NEN [3] plastic shear being even more than twice the plastic shear in the German standard in some cases.

4.2 Materials

Another factor than can influence the response under bending and shear is the constitutive equation of the material. The yield stress f_y and the post yield behaviour are two factors to be taken into account. In order to study the possible influence of the yield stress and the existence of strain-hardening (or lack thereof) four different materials have been simulated. Two steels with perfect plasticity with grades S235 and S355 and two steels with strain-hardening plasticity also corresponding to grades S235 and S355. In the elastic regime, all the different steels have an elastic modulus $E = 210000 N/mm^2$. In order to avoid any convergence problems, the horizontal plateau of the perfect plastic materials have been given a mild slope of $E/10000 = 21 N/mm^2$. For the isotropic-hardening materials, a quad-linear strain-hardening model has been used from Yun and Gardner [21]. Also, the horizontal yield plateau in these materials has been modified and a small hardening $E/10000$ has been introduced. The following figures show the stress-strain behaviour of the steels introduced in *Abaqus*:

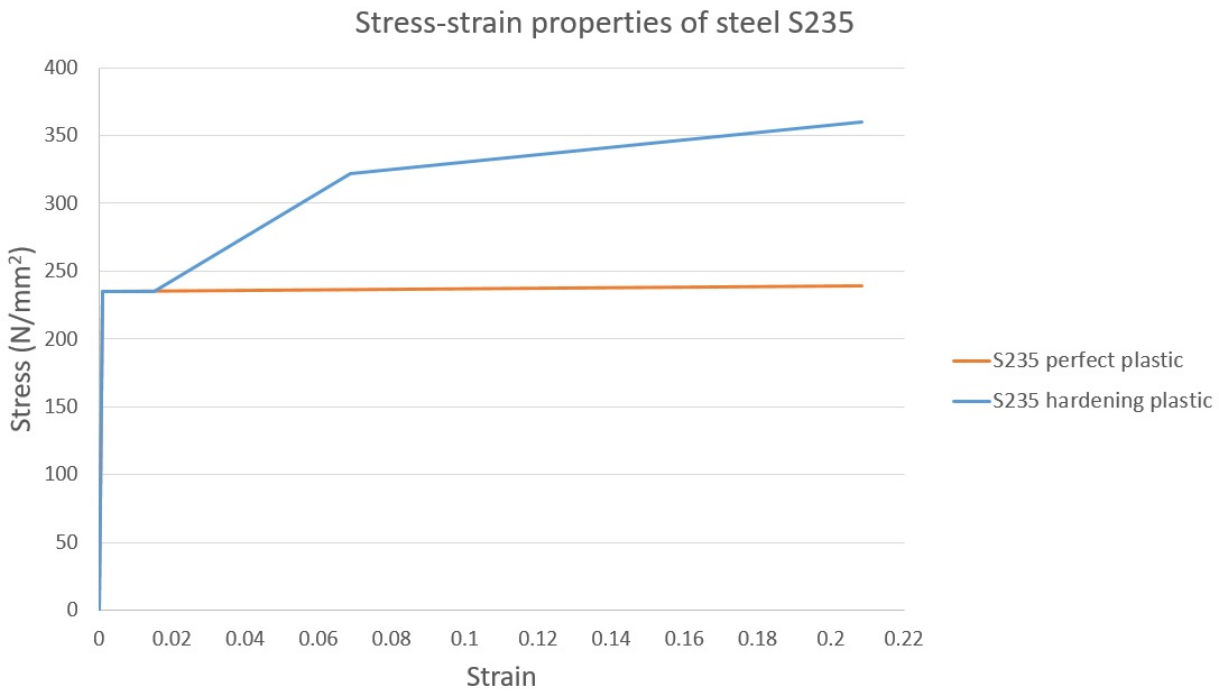

Figure 4.1: Stress-strain curves for steels S235 with perfect plasticity and with strain-hardening

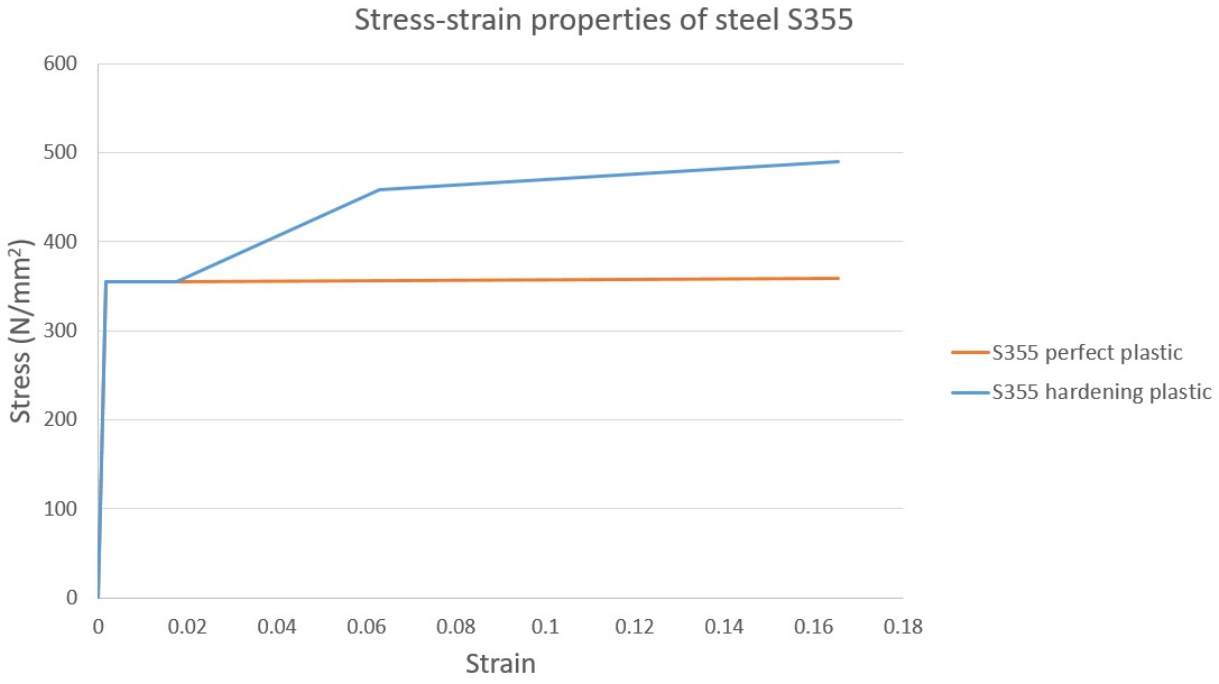

Figure 4.2: Stress-strain curves for steels S355 with perfect plasticity and with strain-hardening

The materials with strain-hardening remain equivalent to their homologous perfect-plastic steels up to the yield plateau. From that point on, the behaviour is different. In the following table all the parameters are given for the hardening steels, where ε_{yp} is the total strain after the yield plateau, E_1 and E_2 are the strain-hardening moduli of the two parts of the hardening regime and C_1 is the ratio between the strain at the point just between the two different hardening regimes and the ultimate strain ε_u. At that strain the ultimate strength is f_u.

Table 4.1: Parameters of the steels with strain-hardening from X. Yun and L. Gardner [21]

$f_y\,(N/mm^2)$	$\varepsilon_{yp}\,(\%)$	$E_1\,(N/mm^2)$	C_1	$E_2\,(N/mm^2)$	$f_u\,(N/mm^2)$	$\varepsilon_u\,(\%)$
235	1.5	1616	0.33	271.3	360	20.83
355	1.74	2283	0.38	302.4	490	16.53

Chapter 5

Results and Analysis

In this chapter, some the results obtained from the 172 simulations are displayed. The results will be sorted by different materials. The simulations have provided with the failure load for every beam (with a given section and span) made of a certain steel with two possible yield stresses and two possible plastic behaviours: perfect plastic or plastic with strain-hardening. These results have been plotted in a series of graphs where these results are compared to the bending-shear interaction design rules in EN 1993-1-1 [1], NEN 6770 [3], DIN 18800 [4] and also the interaction rule in the Eurocode but considering as shear area A_v the area of the web A_w. The utilisation ratios for bending M/M_{pl} and for shear V/V_{pl} at failure are represented for each beam as a point in the charts. Any points laying beneath the interaction curve will be indicating that the rule is more optimistic in those cases than the results have proven. Also, load-deflection curves are displayed as well as comparison Von Mises stresses, strains and deflections for some beams.

5.1 Detailed results for simulations with perfect plastic S235 steel - HEA240

Five beams with section HEA240 and variable span have been simulated in perfect plastic S235 steel. As an example of the output of the model at failure, the following figures display the stresses, strains and deflections of a beam in HEA240 section with span $L = 1400mm$. Fig. 5.1 shows the Von Mises stresses in the beam:

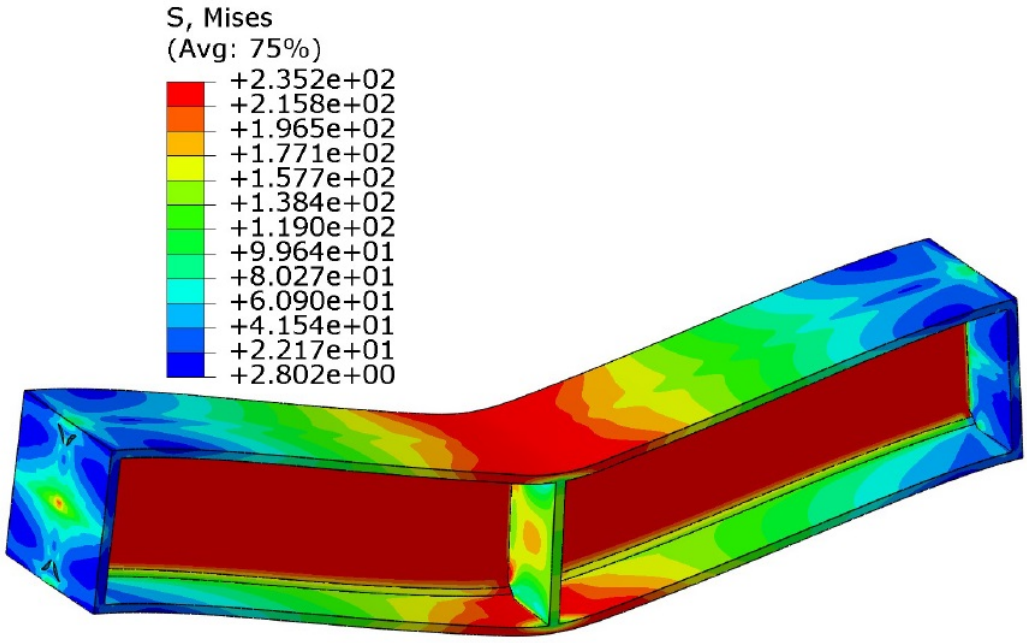

Figure 5.1: Von Mises stresses in an HEA240 beam at failure in N/mm^2. Span $L = 1400mm$.

It is clear that all the web of the beam reaches very high stresses. The beam also has large stresses concentrated around the midsection at the flanges, which indicates the formation of a plastic hinge. Fig. 5.2 shows the longitudinal strains at failure:

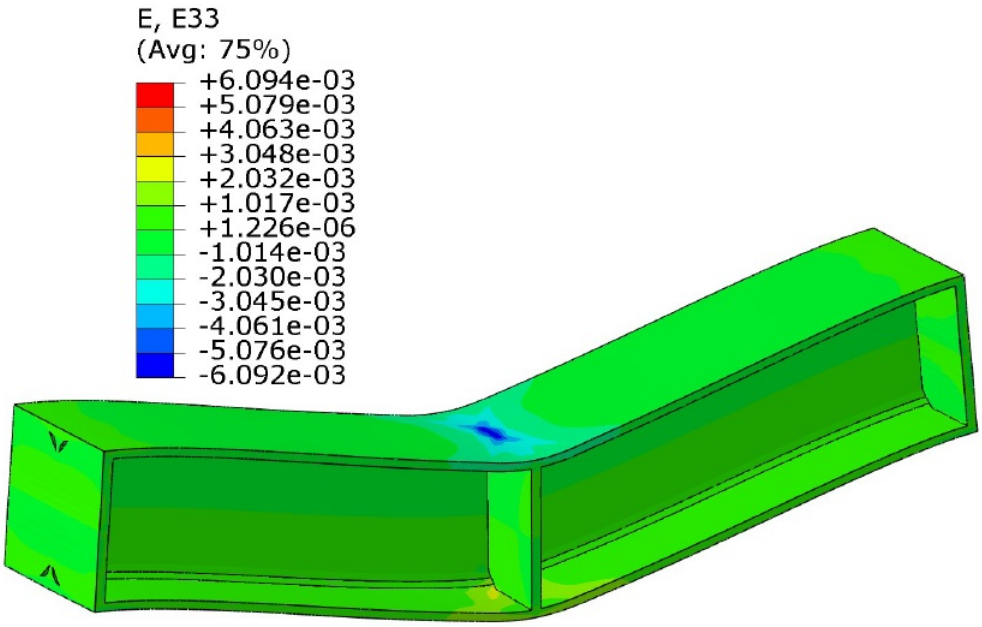

Figure 5.2: Longitudinal strains in an HEA240 beam at failure. Span $L = 1400mm$.

The analysis has been stopped at this load increment because the shear strain is over the maximum allowable strain that has been fixed ($\gamma_{max} = 8\varepsilon_y/\sqrt{3}$):

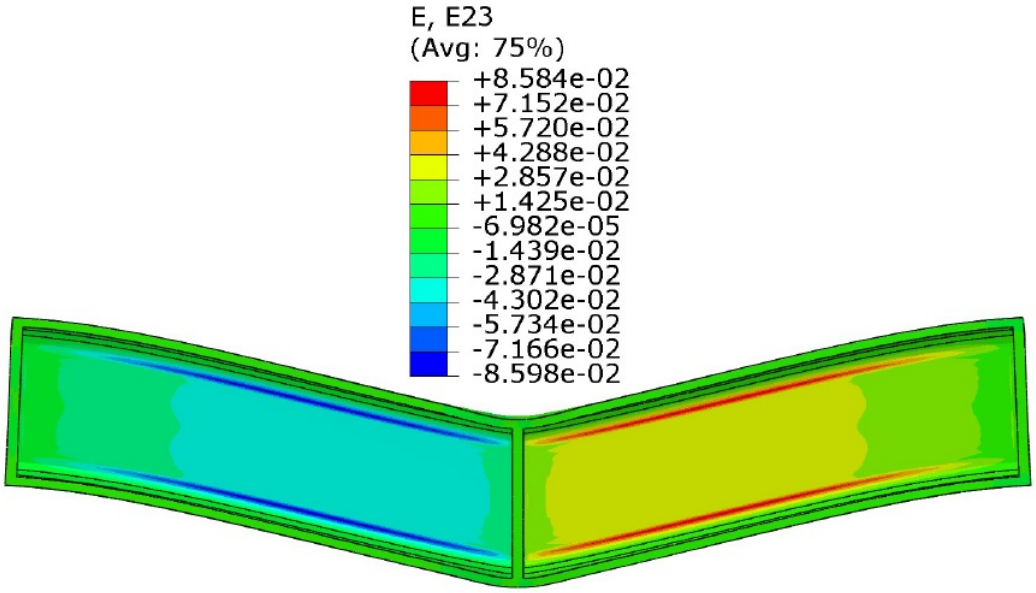

Figure 5.3: Shear strains in an HEA240 beam at failure. Span $L = 1400mm$.

It is clear that shear strains are concentrated in the web, especially around the root area. This concentration of strains around the root area has been consistently seen for the shortest beams where shear force has a more impactful effect. This

type of failure is closer to a shear failure than a bending failure, which ensures a very substantial amount of shear in the interaction. In fig. 5.4 the deflections are displayed. The maximum deflection at failure is $u_{max} = 6.6mm$ which is around $L/200$. The beam is mainly deformating due to shear and not bending:

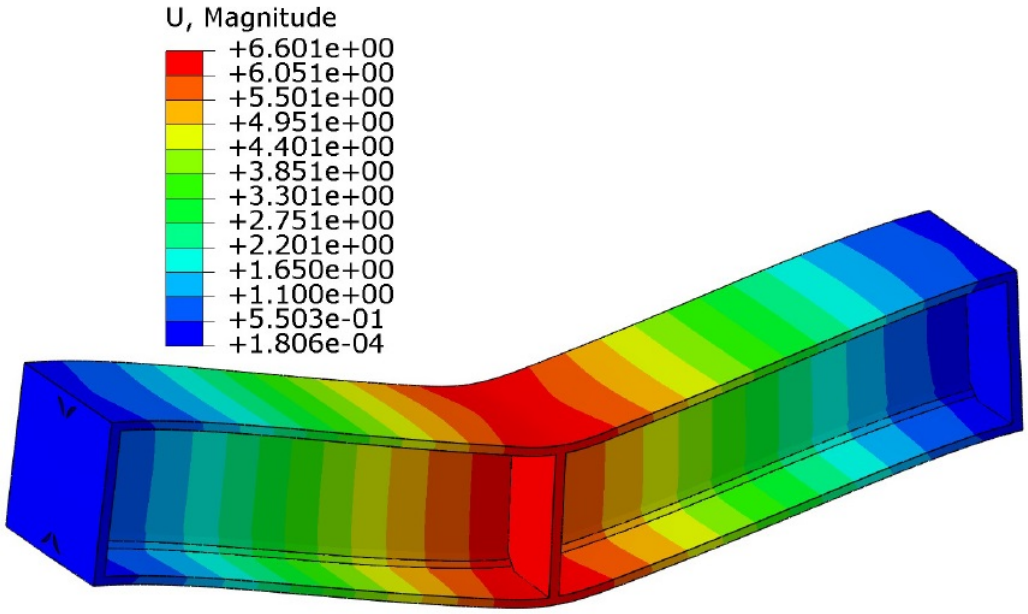

Figure 5.4: Deflections in an HEA240 beam at failure in mm. Span $L = 1400mm$.

For all five HEA240 sections in perfect plastic S235 steel, the same simulations have been performed and similar data have been extracted from the output from *Abaqus*. Then these results have been plotted in order to compare the ultimate failure loads with the interaction rules (fig. 5.6 through fig. 5.9). Also, load-deflection curves are shown. In the following graphs, the legends indicate which span corresponds with each point in the chart. For instance, HEA120_L1800 stands for HEA120 section with span $L = 1800mm$.

:

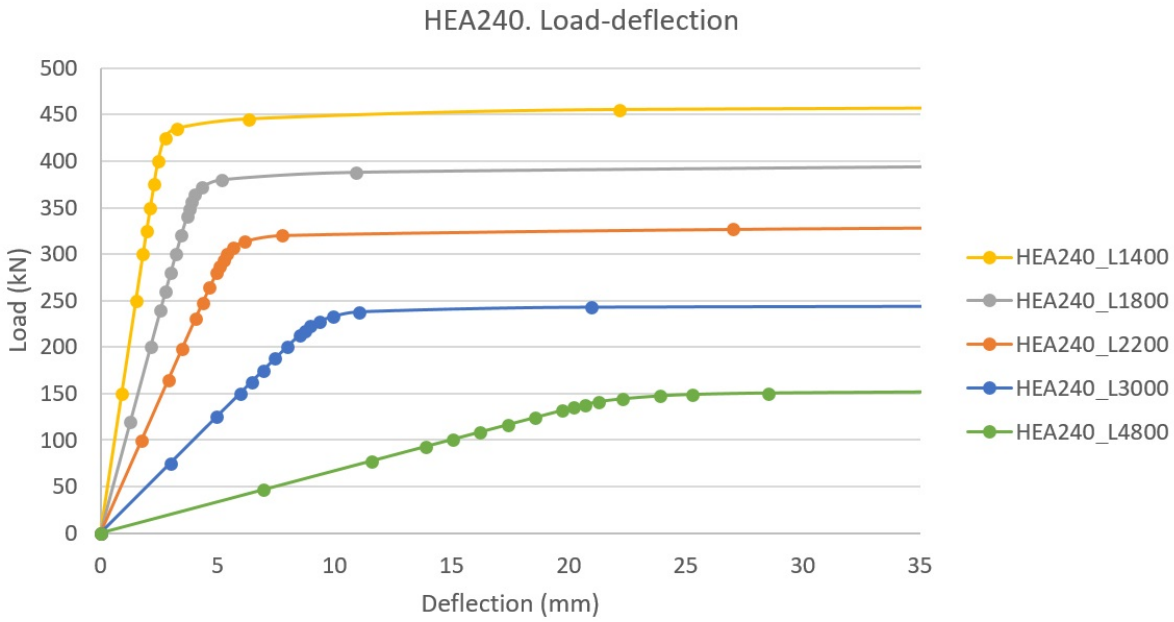

Figure 5.5: Load-deflection curves for HEA240 beams. Perfect plastic S235 steel

It is remarkable that all five beams have a perfectly elastic behaviour for load values somewhat below the ultimate load. When approaching the ultimate load, the linear proportion is lost, and the plastification of the central section starts to occur, with a progressive decrease in the steepness of the curve. After all the central section is yielded, the curve becomes nearly flat indicating the formation of a plastic hinge that rotates freely and a mechanism has formed (note that no strain-hardening is considered in this case). Fig. 5.6 through fig 5.9 show the four interaction rules and the simulated tests results:

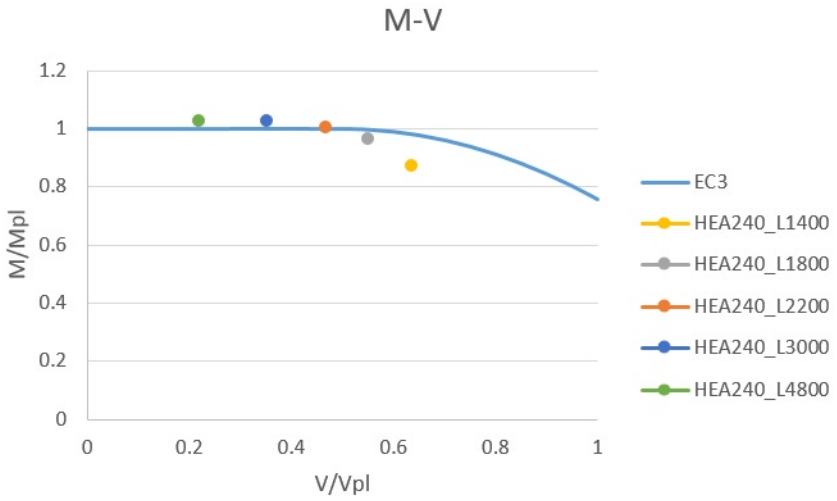

Figure 5.6: Interaction diagram in EN 1993-1-1 [1] and simulated results for HEA240 in perfect plastic S235 steel

It can be observed than two of the tests simulated failed to achieve the resistance stated by EN 1993-1-1 [1] (as indicated in eqs. 2.10 through 2.12. Eq. 2.13 was not used in any case). The shear area used is the one extending up to half way into the flanges (see fig. 2.4). The beams with the shortest spans $L = 1400mm$ and $L = 1800mm$ failed under bending-shear with high shear stresses and strains concentrated in the web. It should also be observed that the shortest beam failed at $0.87M_{pl}$ and $0.64V_{pl}$. This shear level is substantial (a clear bending resistance reduction is noticeable) but not very close to the plastic shear capacity of the section. The adoption of one or another shear area does have an important impact on the interaction. Fig. 5.7 shows the same exact results but adopting the web area (see fig. 2.4) as the shear area:

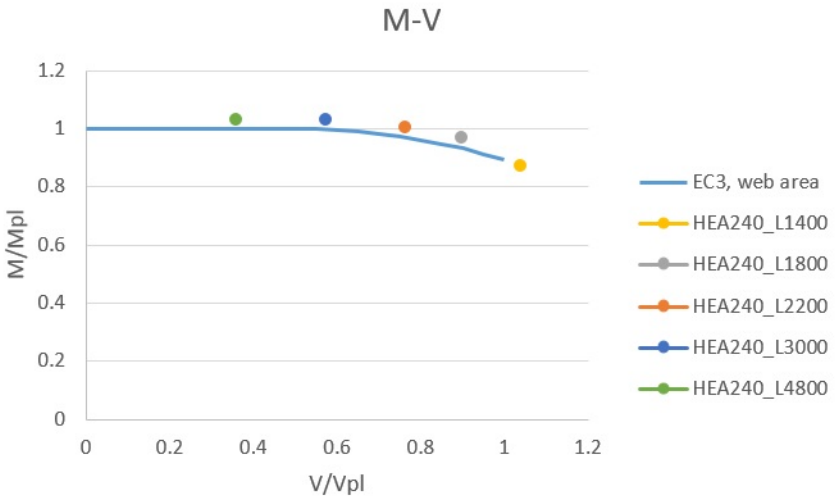

Figure 5.7: Interaction diagram in EN 1993-1-1 [1] using the web area and simulated results for HEA240 in perfect plastic S235 steel

When a more conservative shear area is considered like the web area all points in the graph move towards the right when using the same interaction rule in EN 1993-1-1 [1] (with a higher shear utilisation ratio V/V_{pl} due to lower plastic shear resistance V_{pl}). This makes all tests move above the interaction curve. However, the shortest beam fails at $0.87M_{pl}$ and $1.04V_{pl}$, which indicates shear failure regardless of the level of bending moment in the central section. Notwithstanding, the adoption of the shear area in the Eurocode formulae seems to yield safer results that adjust better to the interaction curve. On the other hand, NEN 6770 [3] considers a larger shear area than EN 1993-1-1 [1] does. The results using the same interaction rule (eqs. 2.10 through 2.12) are displayed in the next figure:

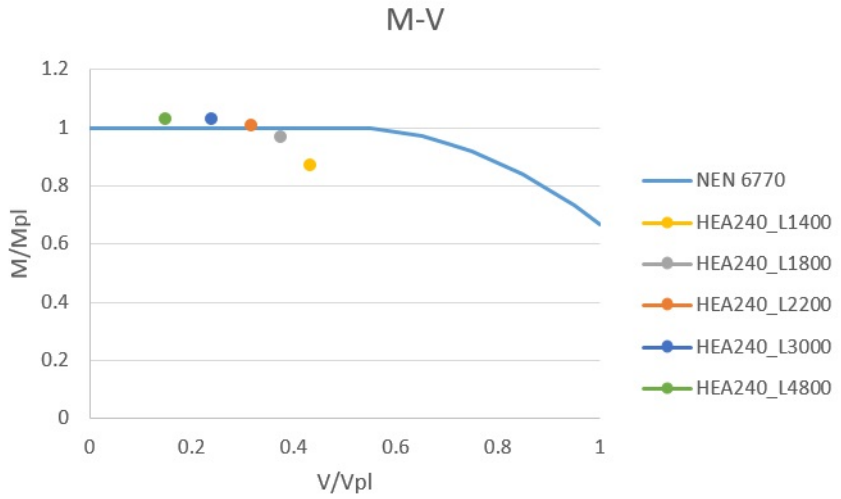

Figure 5.8: Interaction diagram in EN 1993-1-1 [1] using NEN [3] shear area and simulated results for HEA240 in perfect plastic S235 steel

According to NEN 6770 [3], the shortest beam has failed at $0.87M_{pl}$ and $0.43V_{pl}$ not reaching $0.5V_{pl}$. This means that this standard would not consider any reduction of the bending capacity of the beam due to its low amount of shear. However, the resisted moment is $0.87M_{pl}$ which is a significant reduction. The adoption of such a large shear area appears to be unconservative. This interaction rule is again too optimistic for the two shortest beams simulated.

Fig. 5.9 shows the interaction rule in DIN 18800 for the simulated tests for the studied beams with section HEA240. To calculate the bending resistance $M_{V,Rd}$ eq. 2.16 was used.

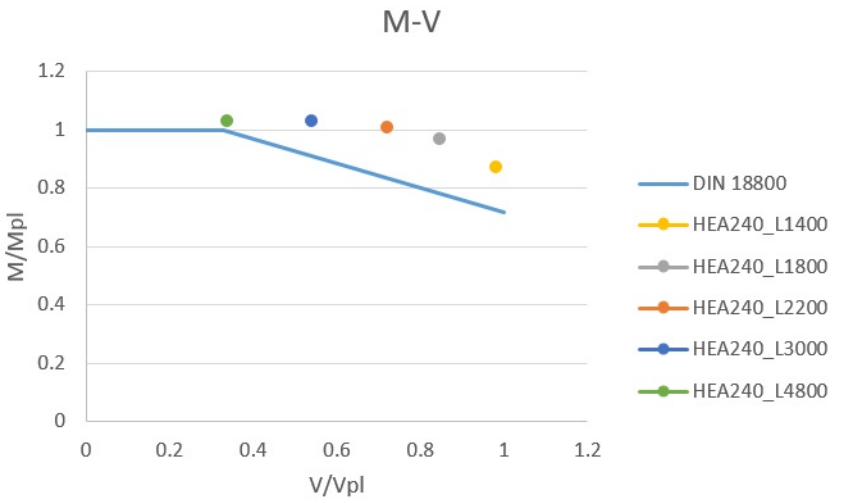

Figure 5.9: Interaction diagram in DIN 18800 [4] and simulated results for HEA240 in perfect plastic S235 steel

All of the simulated tests are on the safe side. The shear area considered in the German norm leads to vey similar shear plastic resistance using only the web area. It is obvious that this norm is more conservative than EN 1993-1-1 [1] when using the web area since most points are much further away from the interaction curve. Also, the interaction starts at $0.33V_{pl}$ and not at $0.5V_{pl}$, which appears to be a bit too conservative from what these particular results show.

5.2 Detailed results for simulations with hardening S235 steel - IPE120

Five beams with section IPE120 and variable span have been simulated in hardening plastic S235 steel. As an example of the output of the model at failure, the following figures display the stresses, strains and deflections of a beam in IPE120 section with span $L = 1200mm; L = 10d$. Fig. 5.10 shows the Von Mises stresses in the beam:

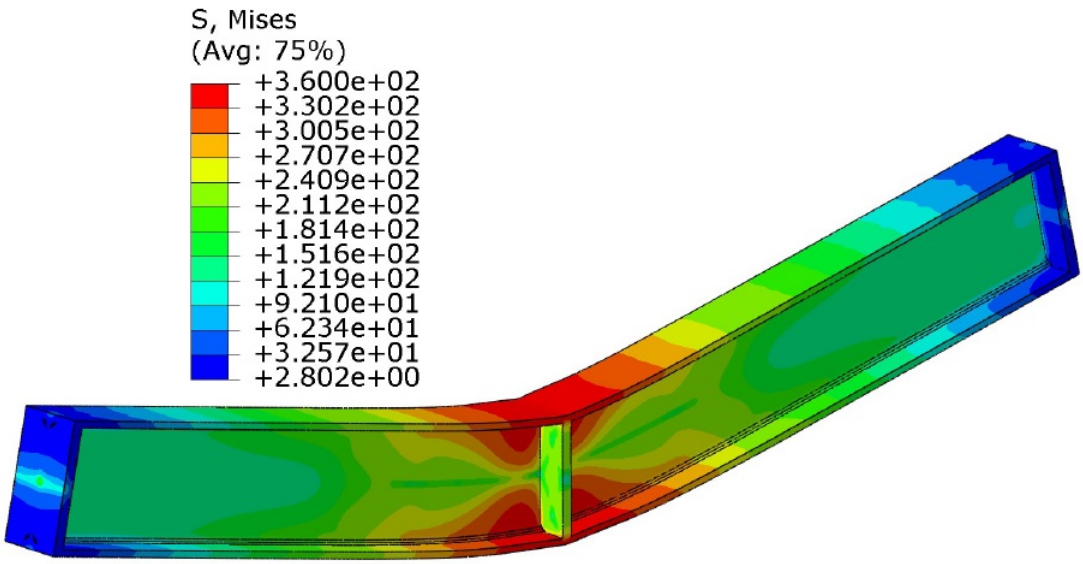

Figure 5.10: Von Mises stresses in an IPE120 beam at failure in N/mm^2. Span $L = 1200mm$.

The beam has large stresses concentrated around the midsection at the flanges, which indicates the formation of a plastic hinge. The web of the beam does not present very large Von Mises comparison stresses in general, just locally at the middle of the beam. This indicates that for this beam with a span $L = 10d$ the shear force has not had a great impact and the interaction is governed by flexure in this case. Fig. 5.11 shows the longitudinal strains at failure:

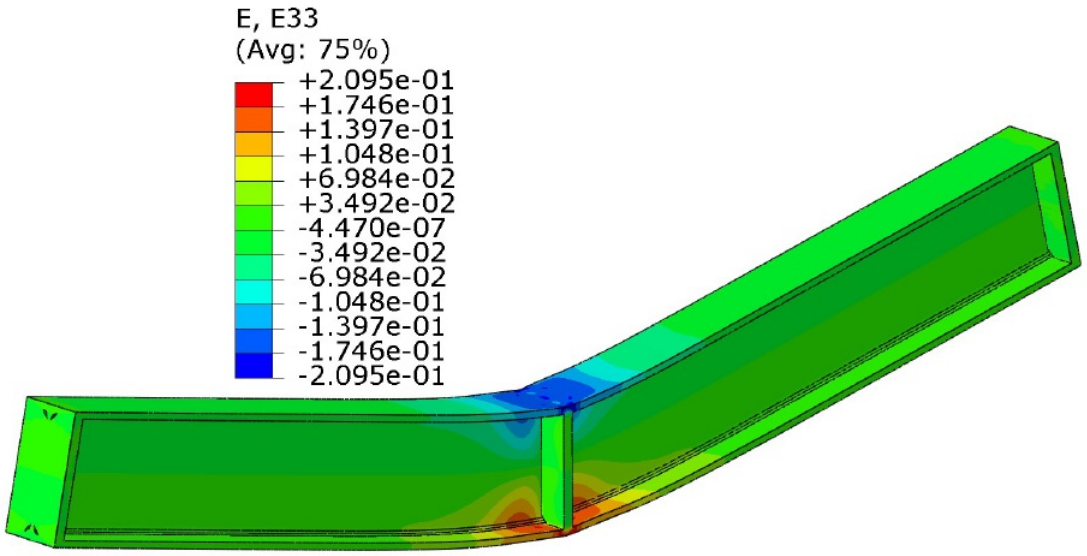

Figure 5.11: Longitudinal strains in an IPE120 beam at failure. Span $L = 1200mm$.

It is clear than strains are concentrated near the center of the beam at the flanges. The analysis has been stopped at this load increment because the shear strain is over the maximum allowable strain that has been fixed:

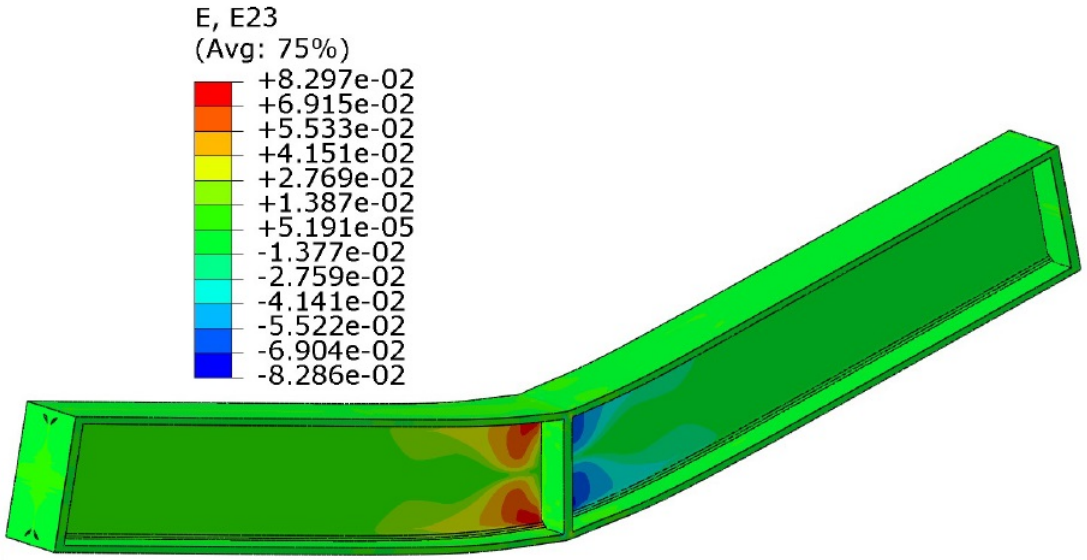

Figure 5.12: Shear strains in an IPE120 beam at failure. Span $L = 1200mm$.

Shear strains are concentrated in the web, especially near the application of the load. However, the rest of the web does not have large shear stresses, which indicates that the red and blue areas in the diagram are mainly due to local effects and the introduction of the concentrated load. This simulation represents the failure of an

IPE120 beam mainly due to bending, with little or no influence of shear on the ultimate resistance of the beam. In fig. 5.13 the deflections are displayed:

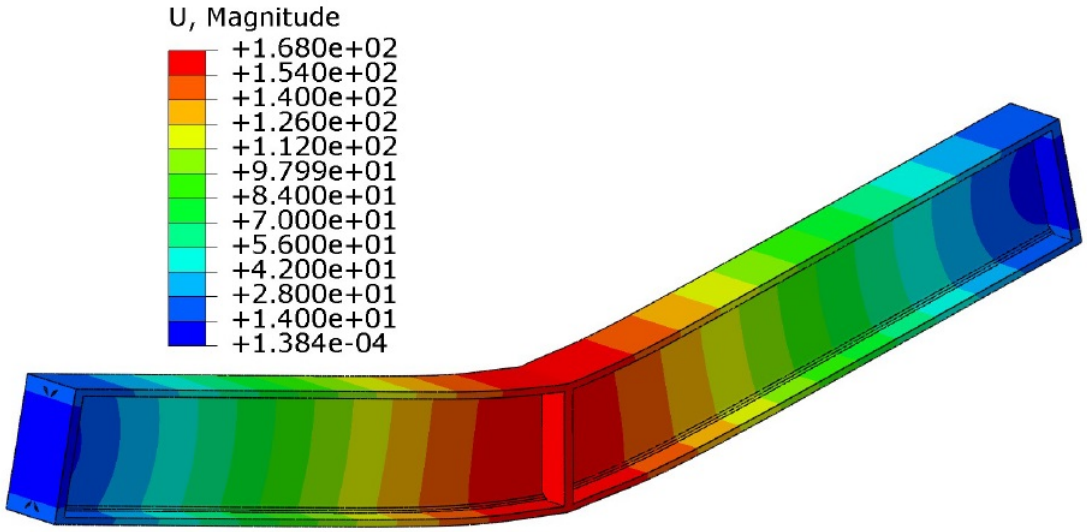

Figure 5.13: Deflections in an IPE120 beam at failure in mm. Span $L = 1200mm$.

The maximum deflection at failure is $u_{max} = 168.8mm$ which is around $L/7$. The beam is definitely undergoing large deformations at this load increment. The maximum deflection is somewhat larger than the depth of the beam itself.

For all five IPE120 sections in S235 steel with strain-hardening, the same simulations have been performed and similar data have been extracted from the output from *Abaqus*. Then these results have been plotted in order to compare the ultimate failure loads with the interaction rules (fig. 5.15 through fig. 5.18). Also, load deflection curves are shown:

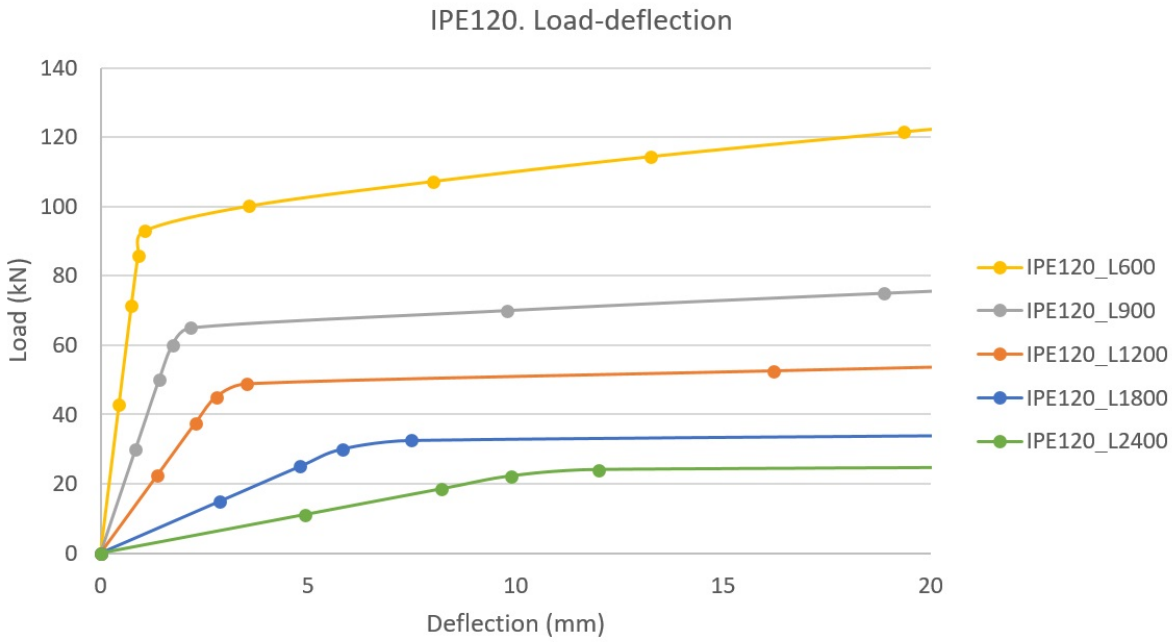

Figure 5.14: Load-deflection curves for IPE120 beams. Hardening plastic S235 steel

As for the case of the HEA240 beams in perfect plastic S235 steel, all five beams have a perfectly proportional behaviour for low load values. However, with a steel with strain-hardening when adding progressively more load the plastification of the central section starts to occur indicating the formation of a plastic hinge, but the curve is not horizontal. This means that the plastic hinge has a certain stiffness, which can carry some more load, up to failure. Fig. 5.15 through fig 5.18 show the four interaction rules and the simulated tests results:

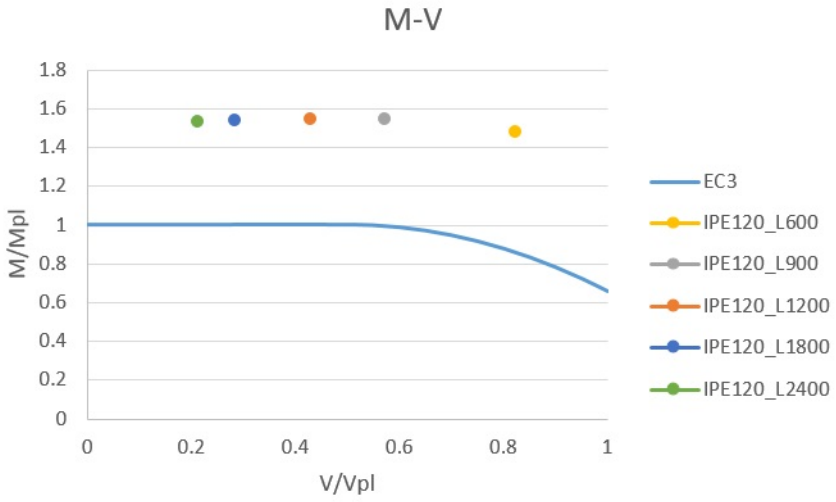

Figure 5.15: Interaction diagram in EN 1993-1-1 [1] and simulated results for IPE120 in hardening plastic S235 steel

It is very obvious that when taking into account the strain-hardening of the steel all the results are very much on the safe side. For the four longest beams, the bending resistance has proved to be almost identical with a value of around $1.54M_{pl}$. For the shortest beam with span $L = 600mm$ the bending resistance has been a bit smaller with a value of $1.48M_{pl}$, which still is considerably safe. Fig. 5.16 shows the same interaction rule but considering only the web area as shear area:

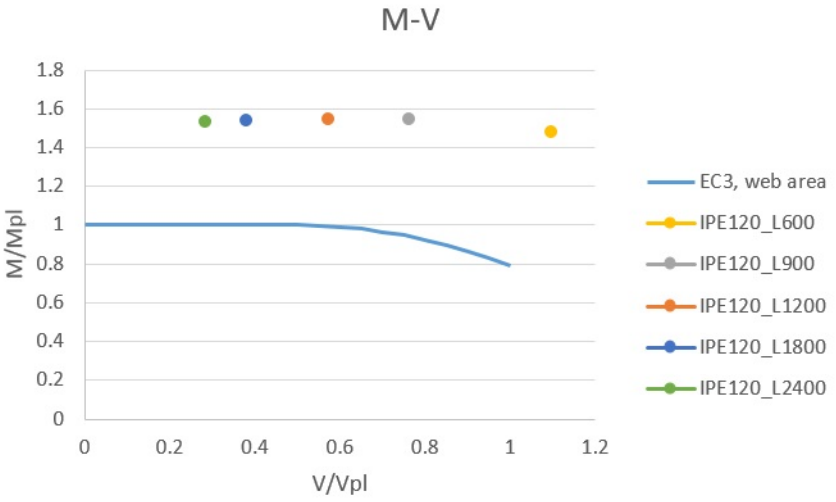

Figure 5.16: Interaction diagram in EN 1993-1-1 [1] using the web area and simulated results for IPE120 in hardening plastic S235 steel

As it can be observed in the results with the HEA240 section, when a more con-

servative shear area is considered all points in the graph move towards the right. Regardless of this obvious fact, all ultimate bending resistances are much higher than the plastic bending moment M_{pl}, which causes all results to be on the safe side irrespective of the shear area considered. NEN 6770 considers a larger shear area than EN 1993-1-1 does and similar observations can be made:

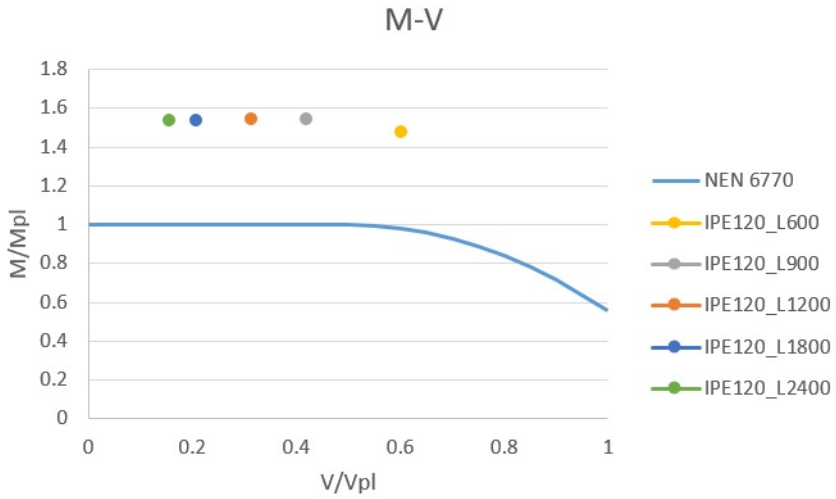

Figure 5.17: Interaction diagram in EN 1993-1-1 [1] using NEN [3] shear area and simulated results for IPE120 in hardening plastic S235 steel

As it has been observed before, the Dutch code may overestimate the shear capacity of the section, which causes all beams to present relatively low shear utilisation ratios with only the shortest beam with a shear ratio higher than $0.5V_{pl}$. It should be noted that the IPE120 beam with span $L = 600mm$ failed at $0.60V_{pl}$ according to NEN 6770 and at $1.10V_{pl}$ if the web area is used with the same formulae, which indicates a shear failure regardless of any flexure.

Fig. 5.18 shows the interaction rule in DIN 18800 for the simulated tests for the studied beams with section IPE120:

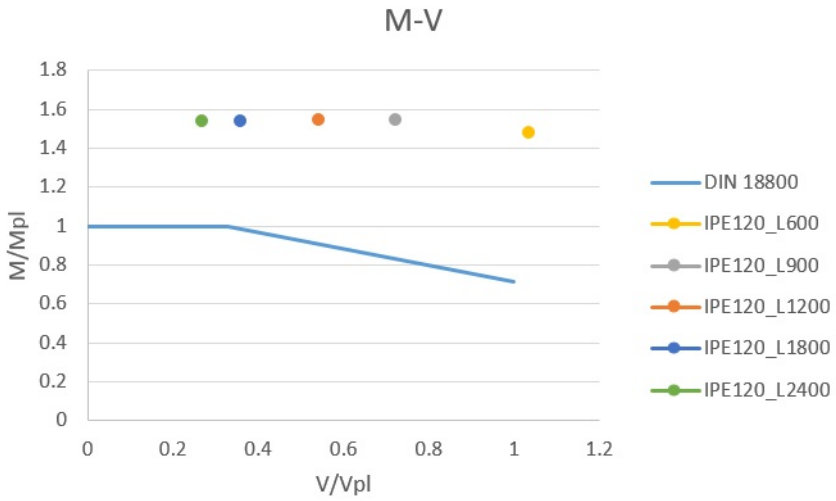

Figure 5.18: Interaction diagram in DIN 18800 [4] and simulated results for IPE120 in hardening plastic S235 steel

Again, the results provided by the German norm and the Eurocode 3 using the web area are very similar with the German standard [4] considering a bit smaller bending resistances.

5.3 Detailed results for simulations with perfect plastic S355 steel - HEA600

The results obtained with perfect plastic steels (S235 and S355) are all very similar. In fact, all the results and failure loads are within a 1% margin of error (or 2% at most). Therefore, most of the observations for the HEA240 section with S235 perfect plastic steel also apply to the same section is S355 steel with perfect plastic behaviour. Likewise, the observations made for the HEA600 section in S355 perfect plastic steel will apply to the same section with lower yield stress. The *Abaqus* output is omitted because it does not provide any additional information and is very similar to the perfect plastic S235 case. Fig. 5.19 shows the interaction rule in Eurocode 3 and the results obtained for an HEA600 in perfect plastic S355 steel:

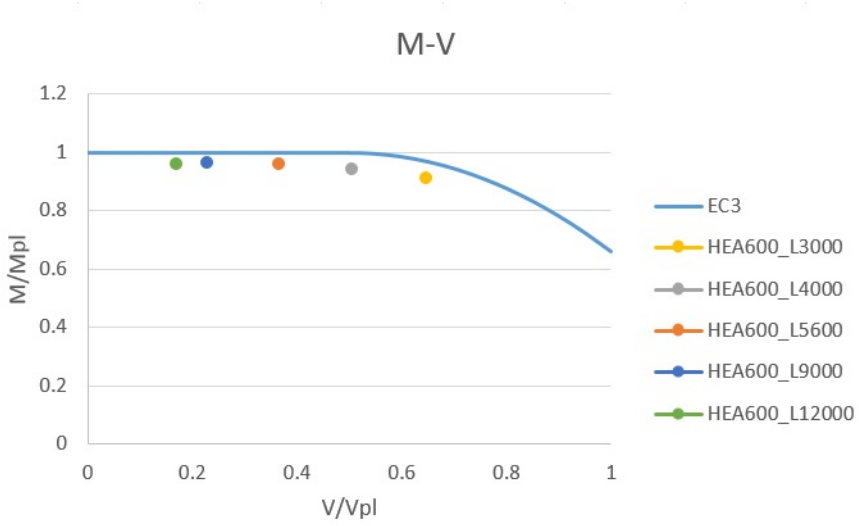

Figure 5.19: Interaction diagram in EN 1993-1-1 [1] and simulated results for HEA600 in perfect plastic S355 steel

It is worth mentioning that this section failed to achieve the plastic bending moment resistance. In fact, the maximum bending resistance achieved was $0.96M_{pl}$ with a minimum of $0.90M_{pl}$ for the shortest beam. HEA600 is a class 1 section when subjected to bending for both S235 and S355, so in theory it should achieve such resistance. This is probably due to the failure criteria adopted. If larger deformations were allowed, higher ultimate loads would be obtained leading to safer results. This has also been seen for the same section in S235 steel:

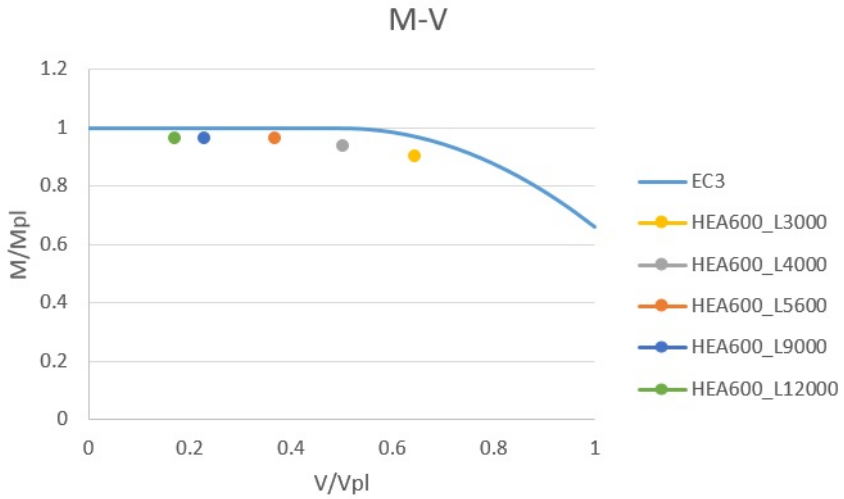

Figure 5.20: Interaction diagram in EN 1993-1-1 [1] and simulated results for HEA600 in perfect plastic S235 steel

The results are almost identical. From what can be seen in fig. 5.19 and fig. 5.20 it appears that HEA600 sections consistantly fail to achieve the plastic bending moment resistance when complying with the maximum deformations established in the failure criteria. However, it can be noted that increasing the shear utilisation ratio does not seem to cause a substancial decrease in bending resistance. Fig. 5.21 shows the interaction in EN 1993-1-1 [1] when using the web area with S355 perfect plastic steel:

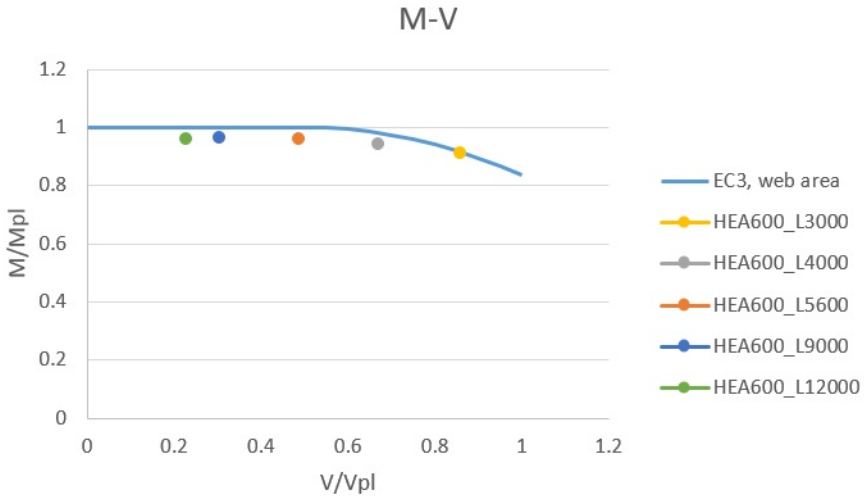

Figure 5.21: Interaction diagram in EN 1993-1-1 [1] using the web area and simulated results for HEA600 in perfect plastic S355 steel

It is curious that in this particular case the only beam in the safe side is the one with highest shear. This is due to the low shear capacity considered in this case. Opposite to this is the rule in NEN 6770 [3]:

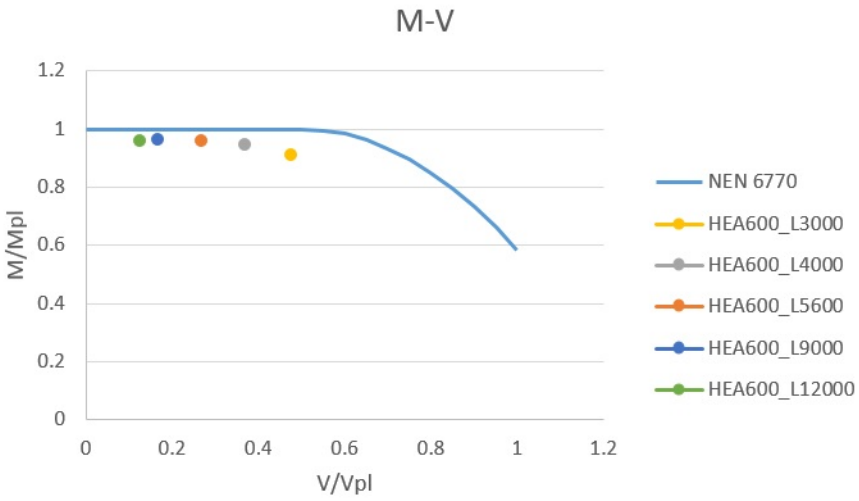

Figure 5.22: Interaction diagram in EN 1993-1-1 [1] using NEN [3] shear area and simulated results for HEA600 in perfect plastic S355 steel

Again, not one of the simulated beams appears to have the minimum shear of $0.5V_{pl}$ in order to account for the interaction. In spite of this, a clear (but not large) reduction in the bending resistance is noticeable for the shortest beam, resisting 6% less bending than the longer specimens. Fig. 5.23 shows the interaction rule in DIN 18800 [4] for the simulated tests for the studied beams with section HEA600:

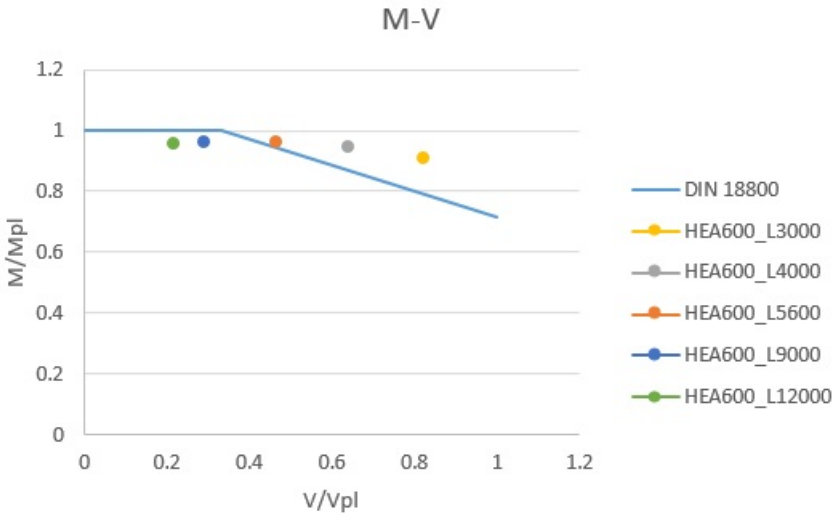

Figure 5.23: Interaction diagram in DIN 18800 [4] and simulated results for HEA600 in perfect plastic S355 steel

5.4 Detailed results for simulations with hardening S355 steel - HEA360

As in the case of HEA600 beams in perfect plastic S355 steel, only the interaction diagrams will be displayed. However, there is a noticeable difference between S235 and S355 when strain-hardening is taken into account. The beams in a higher strength steel present a lower ultimate resistance than the S235 steel beams. Fig. 5.24 shows the interaction rule in EN 1993-1-1 [1] for the hardening plastic S355 beams with section HEA360:

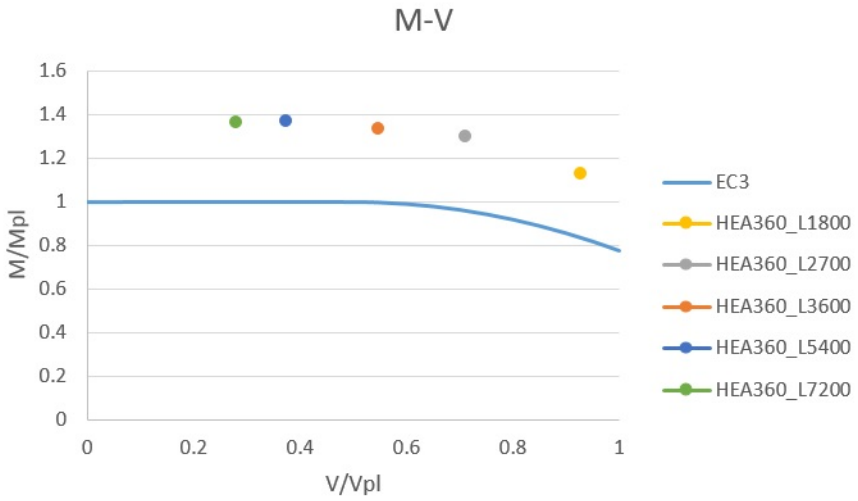

Figure 5.24: Interaction diagram in EN 1993-1-1 [1] and simulated results for HEA360 in hardening plastic S355 steel

And in fig. 5.25 the same beam results are displayed, with hardening S235 steel:

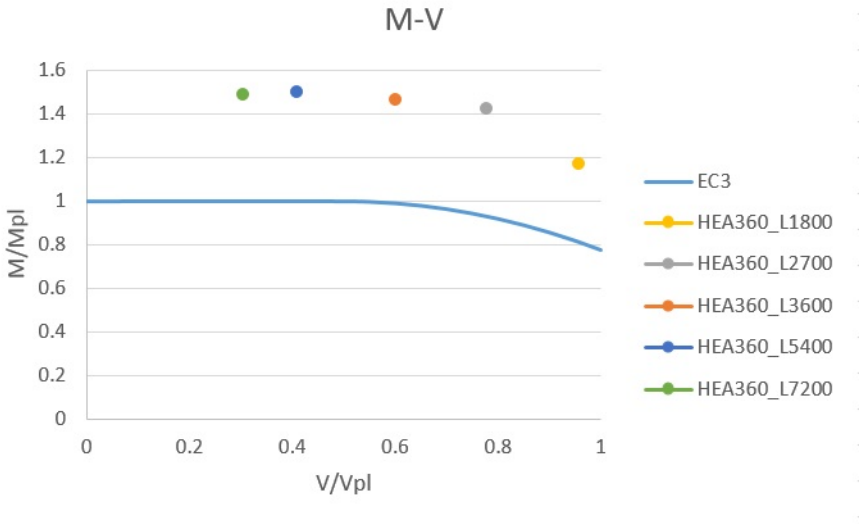

Figure 5.25: Interaction diagram in EN 1993-1-1 [1] and simulated results for HEA360 in hardening plastic S235 steel

It can be noticed that the results for S235 consistently report a higher ultimate strength at failure. The difference in ultimate bending strength for each beam, from longest to shortest have been $0.121M_{pl}$, $0.127M_{pl}$, $0.131M_{pl}$, $0.122M_{pl}$ and $0.038M_{pl}$. For the four longest beams the decrease in strength is quite constant (within a small margin of error) around 12.5%. For the shortest beam, the difference is much smaller around 4%. This fact is repeatedly seen for all sections, with HEA sections presenting smaller ultimate bending resistance differences for the shortest specimens (like the case discussed above) and IPE sections less sensitive to the length of the beam but also reporting different resistances in a consistent manner (possibly the geometries studied were not short enough). These differences were at most around 14% for the longest beams for each section with little or no influence of shear in the failure mechanism.

In fig. 5.26 the same interaction considering just the web area can be seen:

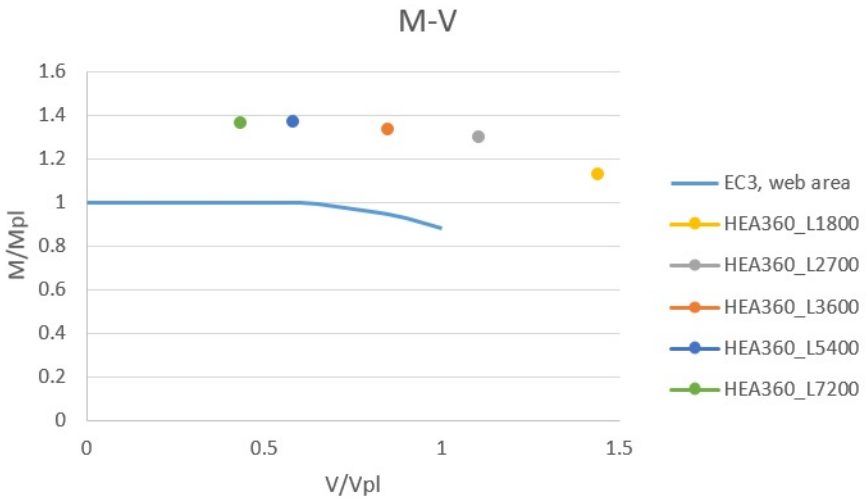

Figure 5.26: Interaction diagram in EN 1993-1-1 [1] using the web area and simulated results for HEA360 in hardening plastic S355 steel

The ultimate shear strength seems to be much higher than $A_w f_y/\sqrt{3}$ with the shortest beam failing at $1.13M_{pl}$ and $1.44V_{pl}$ when the web area is considered. A much higher shear resistance is considered in NEN 6770 [3]:

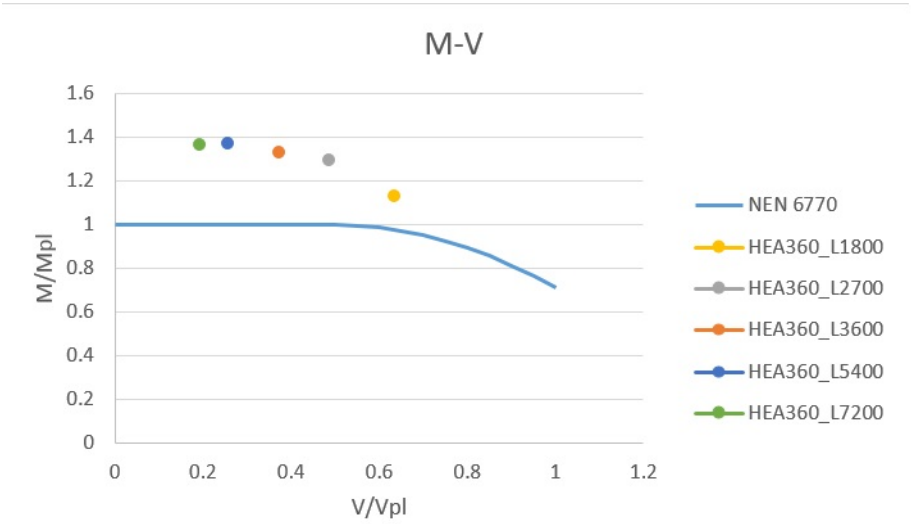

Figure 5.27: Interaction diagram in EN 1993-1-1 [1] using NEN [3] shear area and simulated results for HEA360 in hardening plastic S355 steel

And next figure shows the interaction rule in DIN 18800 [4]. Again, the ultimate shear strength values are similar to those of EN 1993-1-1 [1] when using the web area.

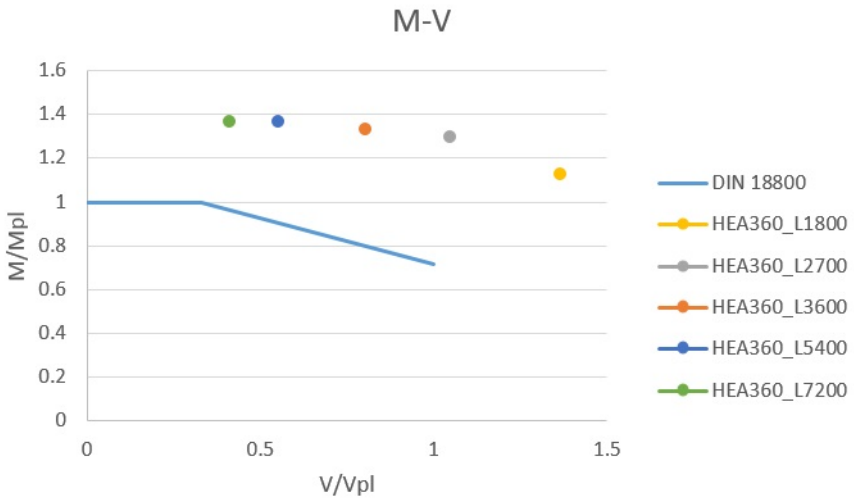

Figure 5.28: Interaction diagram in DIN 18800 [4] and simulated results for HEA360 in hardening plastic S355 steel

5.5 Overview of all the results of the analysis

From the detailed and explicit results in this MSc thesis it is clear that when taking into account the strain-hardening of the steel, all results are very much on the safe side. This means that if large deformations are allowed, all the simulated beams achieve a bending resistance higher than M_{pl} regardless of shear. This is due to the fact that the strain-hardening of the steel provides additional bending resistance. Fig. 5.29 through 5.32 show all the results of beams made of steels with strain-hardening. Note that all the points laying above the interaction curve are on the safe side, while the points below the curve correspond to unsafe predictions.

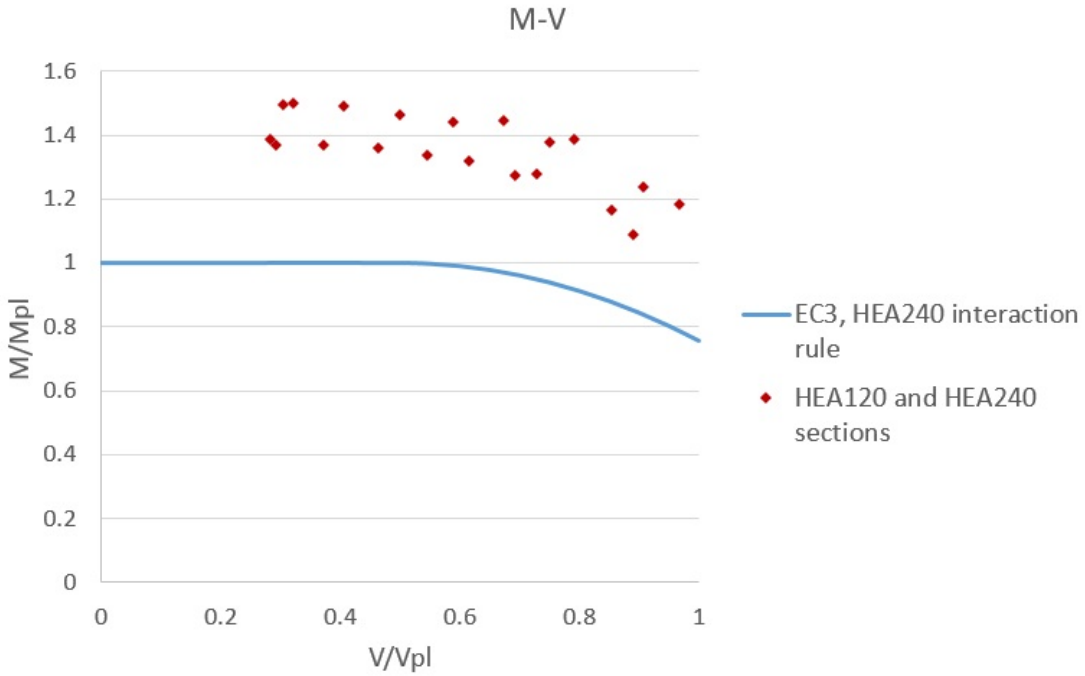

Figure 5.29: Interaction diagram in EN 1993-1-1 [1] for HEA240 and results for all HEA120 and HEA240 beams made of steels with strain-hardening

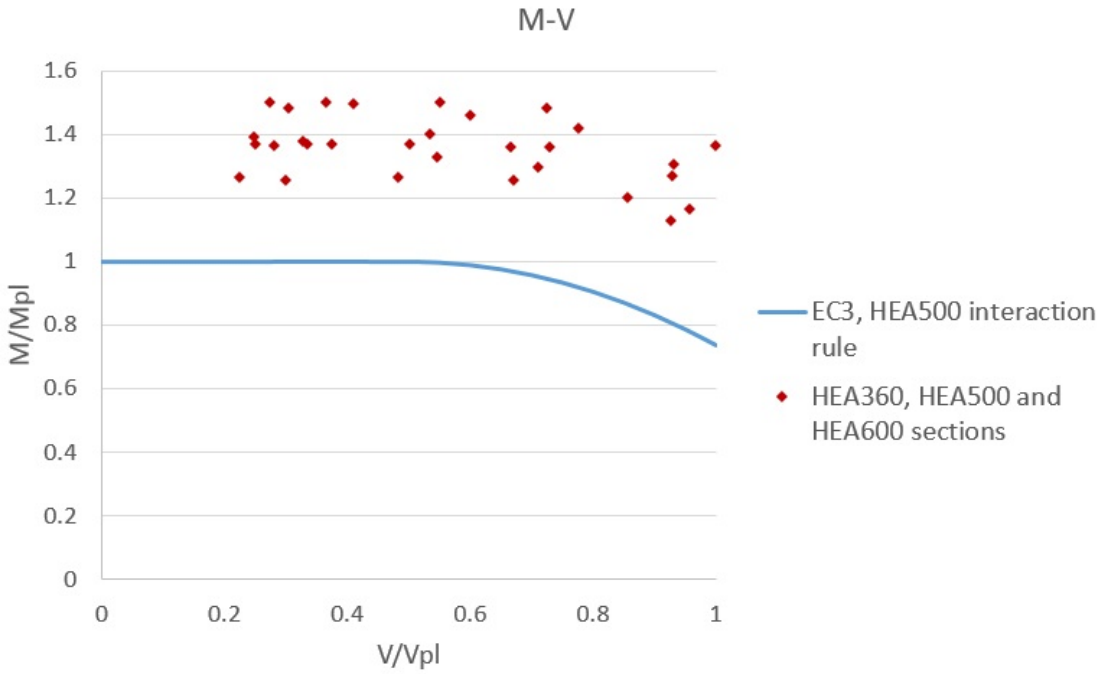

Figure 5.30: Interaction diagram in EN 1993-1-1 [1] for HEA500 and results for all HEA360, HEA500 and HEA600 beams made of steels with strain-hardening

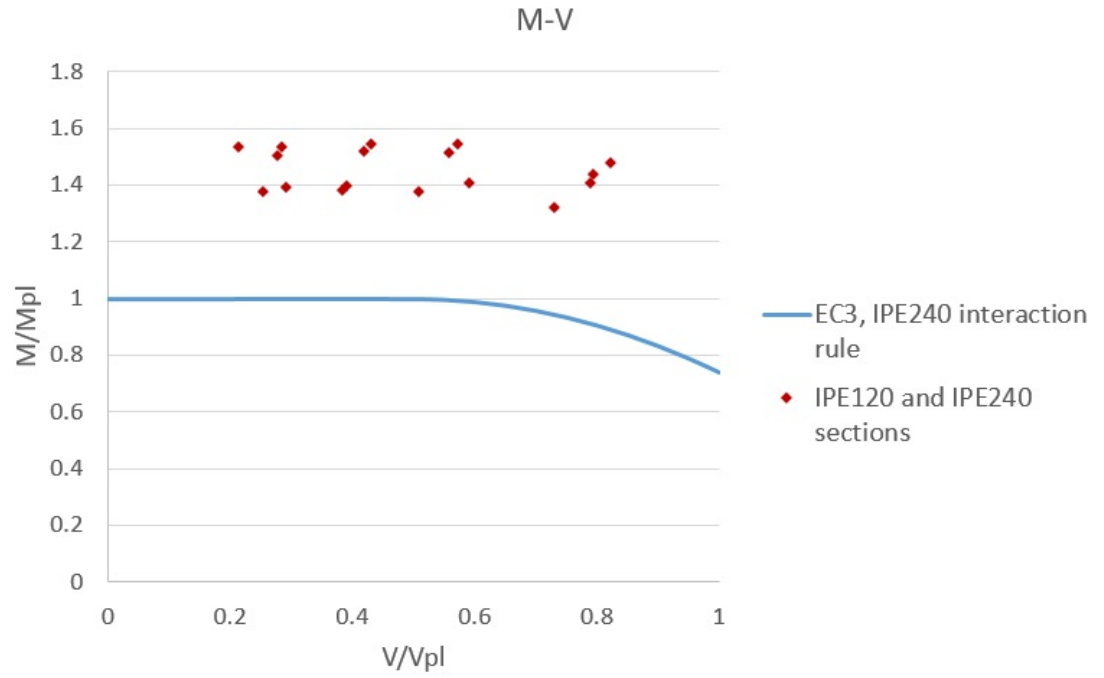

Figure 5.31: Interaction diagram in EN 1993-1-1 [1] for IPE240 and results for all IPE120 and IPE240 beams made of steels with strain-hardening

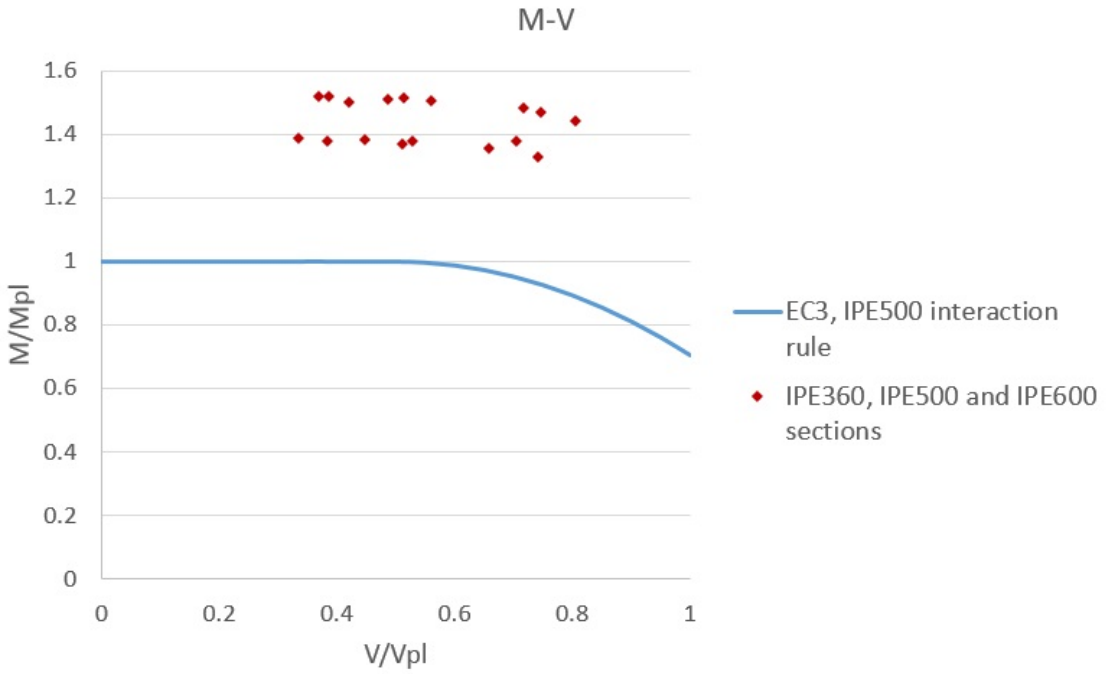

Figure 5.32: Interaction diagram in EN 1993-1-1 [1] for IPE500 and results for all IPE360, IPE500 and IPE600 beams made of steels with strain-hardening

However, for the perfect plastic steels some results are conservative, while others are clearly unconservative. Fig. 5.33 and 5.34 show the results of all the perfect-plastic HEA beams compared to an interaction diagram in EN 1993-1-1 (using the shear area prescribed in the Eurocode):

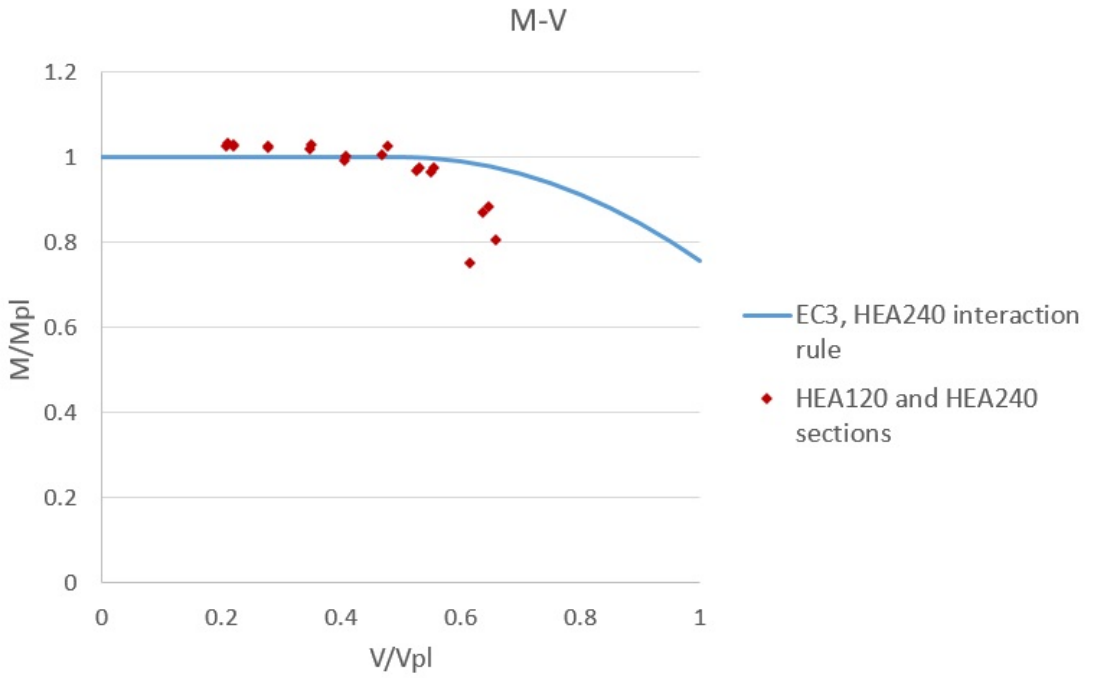

Figure 5.33: Interaction diagram in EN 1993-1-1 [1] for HEA240 and results for all HEA120 and HEA240 beams with perfect plastic steels

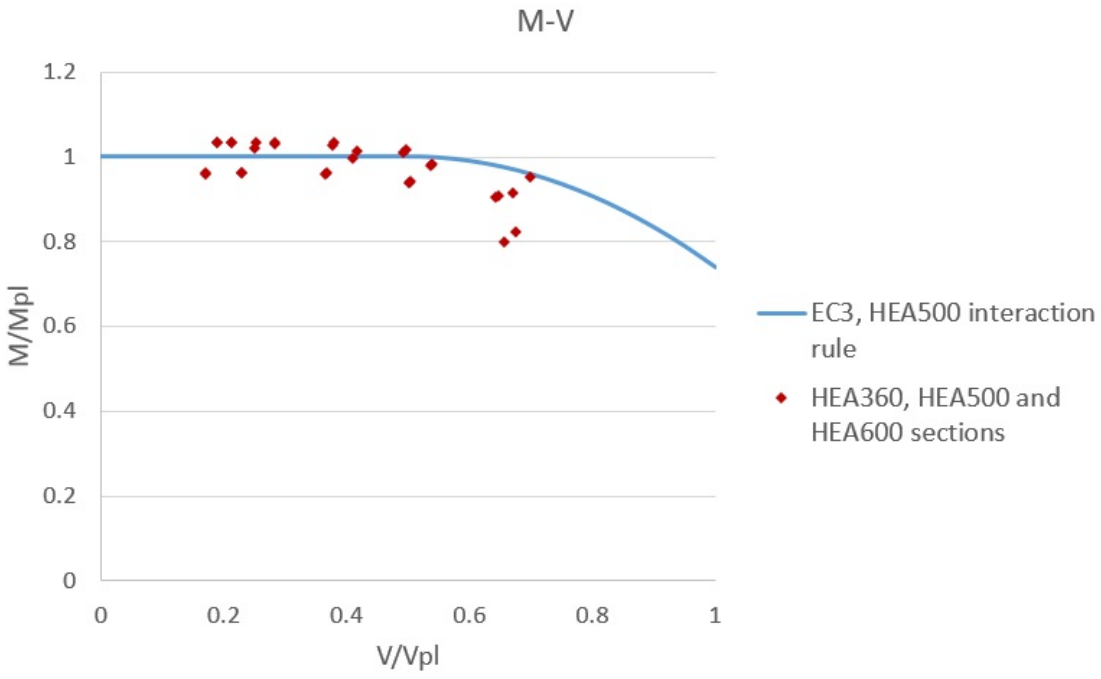

Figure 5.34: Interaction diagram in EN 1993-1-1 [1] for HEA500 and results for all HEA360, HEA500 and HEA600 beams with perfect plastic steels

All the beams tested have sections belonging to class 1 in exception for HEA240 in steel S355. HEA240 is classified as class 2 for steel S355 although the web is class 1. HEA240 beams in S355 behaved similarly to other class 1 sections from the HEA series and for the low shear cases three HEA240 beams reached the plastic bending resistance M_{pl} in perfect plastic S355 steel. In fact, and as it has been mentioned before, the only section that consistently failed to achieve M_{pl} is HEA600 section for both S235 and S355 steels without strain-hardening.

It is obvious that this rule clearly overestimates the resistance of the HEA sections in many cases when the strain-hardening of the steel is not considered. However, IPE sections do not experiment such a dramatical decrease in bending resistance due to shear. Fig. 5.35 and 5.36 show similar diagrams for the IPE section series.

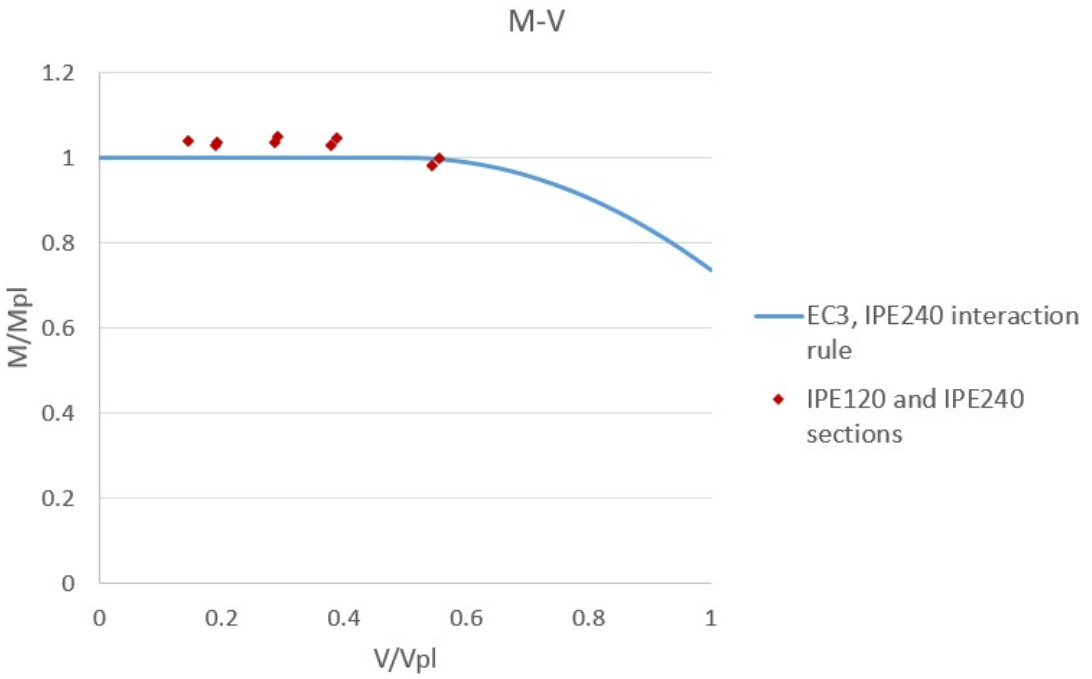

Figure 5.35: Interaction diagram in EN 1993-1-1 [1] for IPE240 and results for all IPE120 and IPE240 beams with perfect plastic steels

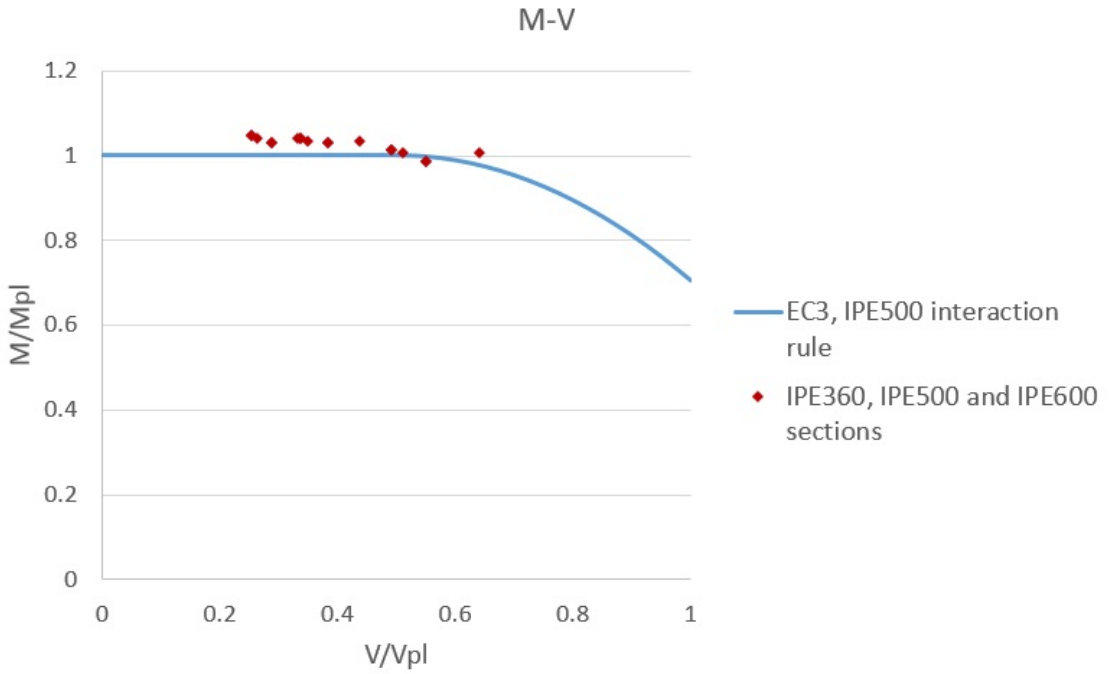

Figure 5.36: Interaction diagram in EN 1993-1-1 [1] for IPE500 and results for all IPE360, IPE500 and IPE600 beams with perfect plastic steels

For the IPE sections, the diagrams are much safer. The loss of bending capacity due to shear seems to be much smaller than the loss of bending resistance for HEA sections.

In order to quantify the accuracy of the interaction rules the utilisation ratios of the beams have been calculated. These ratios are defined as the quotient between the distance from the origin to the point considered and the distance from the origin to the interaction curve, with both distances measured on the same line. As shown in fig. 5.37, the utilisation ratio of the sample is r_u/r_{pred}.

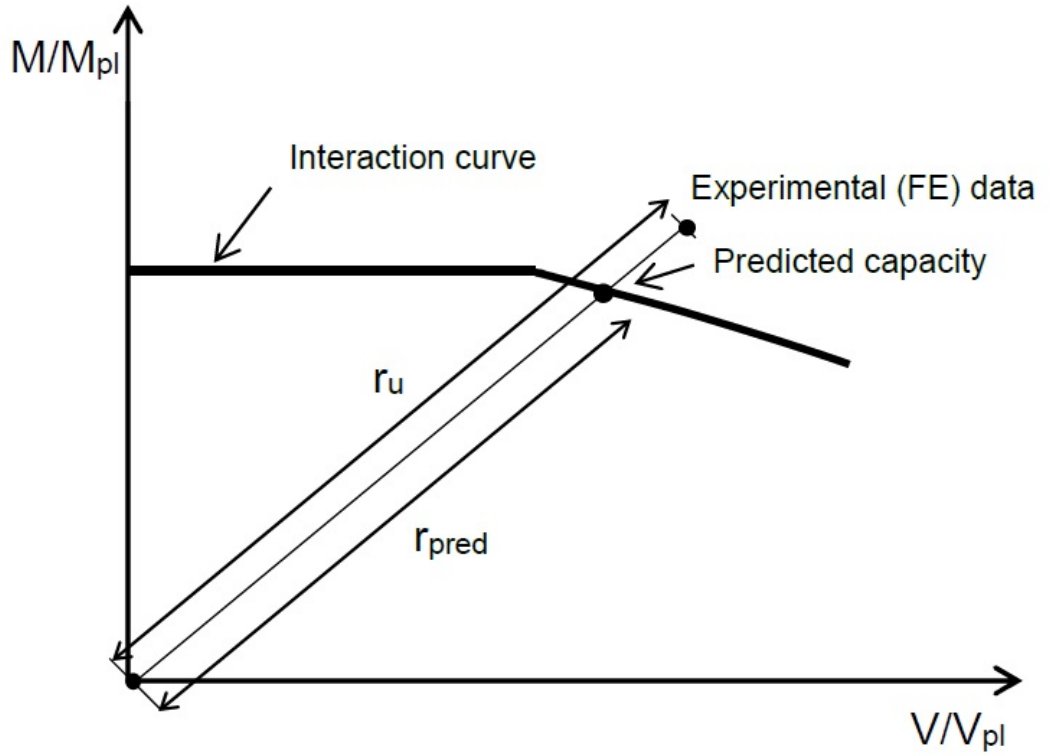

Figure 5.37: Representation of a sample to obtain its utilisation ratio r_u/r_{pred}

The utilisation ratio shows how the results compare to the interaction rule. All utilisation ratios higher than 1.0 indicate that the failure load obtained in the analysis is greater than what the interaction rule considered suggests indicating a safe prediction. Tables 5.1 and 5.2 show the average utilisation ratios of the obtained results for each section with perfect plastic S235 and S355 steels (displayed in fig. 5.33 through 5.36). The four interaction approaches studied are shown separately.

Table 5.1: Average utilisation ratios for the beams tested with perfect plastic S235 steel

Shear area	Profile series	Profile size				
		120	240	360	500	600
EN 1993-1-1	HEA	0.96	0.99	0.98	1.01	0.95
	IPE	1.04	1.02	1.02	1.03	1.03
Web area	HEA	1.02	1.03	1.02	1.03	0.97
	IPE	1.04	1.03	1.03	1.03	1.04
NEN 6770	HEA	0.95	0.98	0.97	1.01	0.95
	IPE	1.03	1.02	1.02	1.03	1.03
DIN 18800	HEA	1.08	1.11	1.08	1.08	1.02
	IPE	1.07	1.08	1.08	1.07	1.07

Table 5.2: Average utilisation ratios for the beams tested with perfect plastic S355 steel

Shear area	Profile series	Profile size				
		120	240	360	500	600
EN 1993-1-1	HEA	0.98	0.99	0.99	1.02	0.96
	IPE	1.04	1.03	1.02	1.02	1.04
Web area	HEA	1.03	1.03	1.03	1.04	0.97
	IPE	1.05	1.04	1.03	1.05	1.04
NEN 6770	HEA	0.97	0.99	0.98	1.01	0.95
	IPE	1.04	1.03	1.02	1.00	1.04
DIN 18800	HEA	1.10	1.12	1.09	1.09	1.02
	IPE	1.08	1.08	1.08	1.12	1.08

In the tables above, all results that failed under a shear force higher than V_{pl} (which ocurred only for the smaller shear areas considered) have been omitted. This has been done because any shear force higher than the plastic shear capacity leads to failure by pure shear and not bending-shear interaction, which is out of the scope of this MSc thesis.

It is very noticeable that some shear areas tend to provide less conservative results than others when no hardening of the steel is considered. The shear areas in the Eurocode 3 [1] and in NEN 6770 [3] provide consistently unsafer results than the web area (using the same interactuion rule for all three). The DIN 18800 [4] interaction rule with a different shear area provides the safest results among all the compared rules in this study. Indeed, only 65.1% of the results were on the safe side using the Eurocode interaction rule (using the shear area prescribed in EN 1993-1-

1 [1]). Using the Eurocode interaction rule and considering the shear area in the Dutch code 62.8% were also on the safe side whilst adopting the web area 90% of the results are on the safe side.

Using the German norm DIN 18800 [4] (that considers a linear interaction and a thin shear area extending up to the middle plane of the flanges) 95.3% of the results were on the safe side. As it can be observed in tables 5.1 and 5.2 all the average utilisation ratios for all sections in both grades S235 and S355 are considerably safe. In fact, the utilisation ratios obtained with the DIN 18800 rule are safer than any of the other three interaction approaches used. It must be noted that the only unconservative results using the German standard are all beams with HEA600 section. As it has been discussed before, this section appears to be unable to develop the plastic moment resistance M_{pl} with the established set of maximum allowable deformations. Less strict criteria need to be used to allow this section to reach M_{pl}.

Another fact to point out from all these data is the clear different behaviour between HEA and IPE sections if the largest shear areas are used (Eurocode 3 and NEN shear areas). When no strain-hardening is considered, using the interaction rule in EN 1993-1-1 [1] with its shear area only 48% of the HEA section results were on the safe side. Opposite to this is the case of the IPE sections with 88.9% of conservative results. All the results for IPE beams (with or without strain-hardening and irrespective of the yield stress considered) have shown very little sensitivity to shear force with very small reduction in bending resistance, if any. Tables 5.1 and 5.2 show that all the average utilisation ratios for IPE sections are equal or greater than 1.0.

Chapter 6

Summary, conclusions and future research on M-V interaction

6.1 Summary

In this MSc thesis, a study on bending-shear interaction is performed. Several recent studies indicate that the current interaction rule in EN 1993-1-1 [1] may be unconservative for cases with high levels of shear. The topic is addressed by means of a finite element analysis performed with the software *Abaqus* in order to reproduce three-point bending tests.

The model developed is capable of simulating I-shaped sections subjected to three-point bending with variable spans, invoking different shear utilisation ratios. Hexahedral reduced-integration linear elements were used in all the simulations. Two elements over the flange and web thicknesses proved to be sufficient after a mesh sensitivity check. It has been observed that the numerical model reliably reproduces the real behaviour of steel beams subjected to three-point bending by means of the comparison between the experimental tests in [2] and the failure loads obtained with the numerical model with the established failure criteria. The numerically determined load for two of the specimens tested in [2] were 104.5% and 96.3% of the experimental failure loads. A total of 172 simulations were undertaken. In these simulations, several different sections are studied, and the influence of the yield stress f_y and strain-hardening is investigated. The failure criteria adopted are expressed in terms of maximum allowable deformations.

The results show that when considering the strain-hardening for steels S235 and

S355 all the results are very much on the safe side, and M_{pl} can be achieved regardless of shear in all the simulated tests. However, when no strain-hardening is considered, some results are safe and some others are unsafe with some rules overestimating the resistance of the section. The shear areas in NEN 6770 [3] and EN 1993-1-1 [1] appear to be the least conservative when using the interaction rule in the Eurocode [1]. However, that rule is reasonably conservative when the web area is used as shear area. The most conservative rule seems to be the German rule in DIN 18800 [4] with a different interaction M-V diagram and shear area.

6.2 Conclusions

The main conclusions that can be drawn from this study are the following:

- The simulated results for the beams made of steels with strain-hardening exhibited an ultimate load much higher than those predicted by the interaction equations. Indeed, all beams reached a bending resistance higher than M_{pl} whatever the shear utilisation ratio V/V_{Rd} was.

- The simulated results for the beams made with perfect plastic steels with no strain-hardening were not always on the safe side for all the interaction rules compared in this study. The consideration of larger shear areas leads to a less conservative interaction rule when using the formulae in EN 1993-1-1 [1]. The German rule [4] appears to be the most conservative of all four approaches, with 95.3% of the results being conservative followed by the formula in Eurocode 3 [1] using the web area with 90% of the results on the safe side. Using the interaction approach in EN 1993-1-1, the Eurocode shear area provided 65.1% of safe results and the shear area in NEN 6770 [3] provided only 62.8%.

- The results for the IPE sections show that this profile series is not very sensitive to shear for the spans considered. Only a few of the shortest IPE beams in non-hardening steel experimented a reduction in bending capacity due to shear, which was less than 3% in all cases. All the IPE beams with span $L \geq 7.5d$ reached the plastic bending capacity of the section M_{pl}. In order to grasp a more noticeable interaction it would be necessary to further reduce the beam spans to obtain higher V/V_{pl} ratios without increasing M/M_{pl}.

- The results for the HEA series suggest that these profiles are sensitive to bending-shear interaction with an important reduction of their bending capacity with high levels of shear for all the materials considered in this study.

The equations in Eurocode 3 using the shear areas in NEN 6770 [3] and in EN 1993-1-1 in clause 6.2 [1] consistently provide unconservative results. For most sections these two approaches present average utilisation ratios smaller than 1.0.

- As a design recommendation, when large strains due to strain-hardening are not allowed, the interaction rules recommended are the DIN 18800 [4] approach and the interaction rule in EN 1993-1-1 [1] considering only the web area as shear area. The German rules provide substantially more conservative results. However, EN 1993-1-1 [1] and EN 1993-1-5 [12] suggest a strain-hardening parameter η that can be used to account for some of the additional resistance beyond the yield stress that the steel can provide. The recommended value in EN 1993-1-5 [12] for steels grade S460 and lower is $\eta = 1.2$. This parameter does not increase bending resistance, but provides a greater shear resistance V_{pl} than considering exclusively the web area in that rule. It has been shown that the resistance of I-shaped cross-sections when strain-hardening is considered is greatly increased, and the adoption of a slightly larger shear area than the web area provides more accurate results.

6.3 Future research on bending-shear interaction

In this MSc thesis a study on class 1 and 2 beams subjected to three-point bending has been undertaken. However, there are some limitations to the study.

The conclusions derived from this study only apply to the specific sections considered, which are all doubly symmetric. Further research is needed for mono-symmetric cross-sections such as I-sections with non-symmetric flanges, T-sections or channel sections. Another fact to take into consideration is that all the simulated tests are subjected to uniaxial bending about the major axis. In case of minor axis bending or biaxial bending with bending moments about both principal axes and shear forces acting on the section the conclusions extracted in this study might not be accurate. Specific investigation is required in that regard.

In the case of combined bending, shear and axial force, EN 1993-1-1 [1] does not provide clear directions on how to account for the presence of shear and axial forces. It is not specified which bending reduction has to be calculated in the first place before further reducing it due to the other force. This matter should be addressed by another line of investigation.

Another of the limitations of this study is the applicability of the conclusions to sections belonging to class 1 and 2 only. Semi-compact sections are not addressed in this MSc thesis. More research on these sections should be performed to possibly obtain more favourable expressions than the Von Mises yield criterion for class 3 sections. Also, more research on slender class 4 sections need to be performed to assess the influence of local and shear buckling on the M-V interaction.

References

[1] *Eurocode 3: Design of steel structures - part 1-1: General rules and rules for buildings*, European Comitee for Standardisation, Brussels 2011.

[2] H.H. Snijder and R.W.A. Dekker. Bending-shear interaction of i-shaped cross-sections. *Eurosteel 2014*, 2014.

[3] *NEN 6770, TGB 1990 - Steel structures - Basic requirements and basic rules for calculation of predominantly statically loaded structures*, 2011.

[4] *DIN 18800-1: Steel structures - part 1: Design and construction.* Berlin, 2011.

[5] *Instrucción de Acero Estructural*, Ministerio de fomento, 2011.

[6] K. Basler. Strength of plate girders under combined bending and shear. *Journal of the Structural Division - ASCE*, 87:181–197, 1961.

[7] T. Fujii, Y. Fukomoto, F. Nishino, and T. Okamura. Research works on ultimate of plate girders and japanese provisions on plate girder design. *Proceedings of Colloquium on Design of Plate and Box Girders for Ultimate Strength, London: IABSE*, March 25-26:21–48, 1971.

[8] M. Herzog. Ultimate static strength of plate girders from tests. *Journal of the Structural Division - ASCE*, 100(5):849–864, 1974.

[9] F. Shahabian. The resistance of plate girders to combined shear and patch loading (phd thesis). *School of Engineering, University of Wales, Cardiff*, 1999.

[10] F. Shahabian and T.M. Roberts. Behaviour of plate girders subjected to combined bending and shear loading. *Scientia Iranica*, 15(1):16–20, 2008.

[11] F. Sinur and D. Beg. Moment-shear interaction of stiffened plate girders - numerical study and reliability analysis. *Journal of Constructional Steel Research*, 88:231–243, 2013.

[12] *Eurocode 3: Design of steel structures - part 1-5: Plated structural elements*, European Comitee for Standardisation, Brussels. 2011.

[13] B. Braun. Stability of steel plates under combined loading (phd thesis no. 2010-3). *Institute for Structural Design, Universität Stuttgart*, 2010.

[14] S. Lee, D. Lee, and C. Yoo. Flexure and shear interaction in steel i-girders. *Journal of Structural Engineering*, 139(11):1882–1894, 2013.

[15] *LFRD Bridge Design Specifications, AASHTO*, 2014.

[16] *Specifications For Structural Buildings, AISC*, 2005.

[17] R.W.A. Dekker, H.H. Snijder, and J. Maljaars. Numerical investigation into strong bending-shear interaction in rolled of i-shaped cross-sections. *The International Colloquium on Stability and Ductility of Steel Structures, Timisoara, Romania*, 2016.

[18] B. Jáger, B. Kövesdi, and L. Dunai. I-girders with unstiffened slender webs subjected by bending and shear interaction. *Journal of Constructional Steel Research*, 131:176–188, 2017.

[19] I. J. Baláž and Y. P. Koleková. Resistance of cross-sections to bending-shear-normal force interaction. *Eighth International Conference on Advances in Steel Structures, Lisbon, Portugal*, 133:36–46, 2015.

[20] *Abaqus 2016 Online Documentation, Dassault Systèmes*, 2016.

[21] X. Yun and L. Gardner. Stress-strain curves for hot-rolled steels. *Journal of Constructional Steel Research*, 133:36–46, 2017.